Final Report
Contract NAS8-26007

The Role of Process History, Phase Morphology and Interface Strength Upon the Mechanical Properties of Dispersion-Strengthened Alloys

Period May 27, 1970- May 27, 1972

Principal Investigator

George S. Ansell

December 1972

for George C. Marshall Space Flight Center
National Aeronautics and Space Administration
Marshall Space Flight Center, Alabama 35812

ABSTRACT

The study reported herein was directed towards providing an analytical rationale for the sensitivity-insensitivity of dispersion-strengthened systems to process history. In particular, the research was focussed upon the influence of the particle-matrix interface bond in TD-Nickel and TD-Nichrome of these alloys, and the manner in which the differences in both elastic constants and thermal expansion coefficients between these phases stress this interface when these alloys are subjected to mechanical and thermal loads, upon the mechanical properties of these alloys.

Tests were made of the tensile and compressive yield strength behavior of TD-Nichrome in order to determine if a strength differential, as has been observed for some heats of TD-Nickel, existed for this alloy. No such differential was observed.

The relative bond strengths between the dispersed thoria particles in TD-Nickel and TD-Nichrome were qualitatively determined by comparing the nature of void formation during cold rolling. It was found that the bond strength in TD-Nichrome was higher than for TD-Nickel.

Using a thermal shock method, the bond strength in TD-Nichrome was quantitatively measured and found to be approximately 4 times that for TD-Nickel.

Preloaded samples of TD-Nickel and TD-Nichrome were subjected to a series of high temperature rapid thermal cycles to ascertain the effect of thermal shock on their room temperature mechanical properties. Thermal shock had little effect on TD-Nickel whereas TD-Nichrome showed a significant drop in room temperature yield strength following thermal shock.

The effect of thermal cycling on high temperature behavior was also studied. Here preloaded specimens of TD-Nickel were tested in creep and stress rupture as a function of initial heating rate. Those specimens heated rapidly to temperature, 5,500°F/sec. to 1100°F, exhibited much faster creep rates and shorter rupture lives, than those heated to temperature using shlower heating rates, 55°F/sec.

In connection with these studies a specimen stage was constructed which permited the in situ straining of thin foil specimens within a tilt and rotation stage of an electron microscope. This device permitted the application of strain on the

specimen while still allowing capability for specimen tilt and rotation for specific diffraction conditions.

Finally analytical treatments were made of the stress distribution at the interface and into the sorrounding matrix about second phase particles in two phase alloys as a function of differences in elastic constants and thermal expansion differences between the phase and the application of stress and temperature. These are applied to the effects of these variables upon interface failure and dislocation motion within the alloy.

INTRODUCTION

Dispersion strengthening has been known for many years as a method of considerably increasing the high temperature stability and mechanical properties of numerous alloy systems. Recent effort towards the successful application of this technology has been concentrated on the development of nickel and nickel base alloys strengthened by the presence of finely dispersed thoria particles. However, many problems exist in this system which prevent extension of this technology to other systems and are difficult to resolve on either the basis of prior experience, present technology, or current theory. Unlike some other systems, the nickel base-thoria group appears to be sensitive remarkably to the deformation and thermal cycles used both in the final steps of powder consolidation and in subsequent forming operations required to produce specific shapes.

This research effort was directed towards providing an analytical rationale for the sensitivity-insensitivity of dispersion-strengthened systems to processing history.

In particular it was intended to determine the role of thermo-mechanical processing, dispersed phase morphology and the matrix-dispersed phase interface character upon both the tensile and creep behavior of TD-Nickel and TD-Nichrome alloys.

Previous work had indicated that the underlying basis responsible for this sensitivity to process history, particularly for dispersion-strengthened alloys, may lie in the decohesion of the particle-matrix interface under conditions that subject this interface to high normal tensile stresses. In the simplest case, elastic constant discontinuities between the different phases in the alloy can lead to such high interface stresses when these alloys are loaded.[1] Differences in the thermal expansion coefficients for the different phases present can also produce high interface stresses when the alloy is heated.[2] In this vein, the combination of load, thermal and deformation history together with particle morphology and interface strength would dictate the conditions under which interface failure would be expected.

Unfortunately, our understanding of this problem has been limited. While the interface strength of TD-Nickel has been recently determined,[2] no such data for TD-Nichrome has been obtained. Similarly, although analyses have been made of the particle-matrix interface stresses generated as the result of uniaxial loading[1] and thermal shock[2] this work has not been extended to the study of the effects of superimposed stress and

thermal cycling as would be expected both in the processing and application of these alloys. It is the purpose of this program to determine the interface strength in TD-Nichrome and to study the interrelationship between interface strength and thermal and stress cycling on the mechanical behavior of TD-Nickel and TD-Nichrome alloys.

Several investigators have reported that the yield strength of some alloys is higher in compression than in tension.[1-5] This phenomenon, called the strength differential, or SD effect, is not well understood, but it is believed that the mechanical responsible for the SD effect could be an important key to understanding the yielding behavior of these alloys.

The majority of the data available on the SD effect is related to ferrous alloys, primarily to martensitic steels.[2-4] The SD effect, however, is not limited to ferrous alloys. Several years before the above observations were made, Feisel[5] measured a large SD effect (up to 50%) in a dispersion strengthened nickel-base alloy. More recently, Olsen and Ansell[5] reported a strength differential in TD-Nickel and TD-Nichrome.

A question has arisen as to the mechanism responsible for the strength differential, and several models have been proposed[1,2,6-9]. Of these, the only mechanism which is not uniquely applicable to ferrous alloys has been proposed by Olsen and Ansell.[1] They have postulated that the SD effect is a property associated with two-phase alloys alloys in which the second phase consists of a dispersion of fine, hard, particles. In this case a week particle-matrix interface could lead to an anomalously low yield strength in tension. Here, the yielding behavior of some dispersion strengthened alloys would be sensitive to the magnitude and direction of normal stresses as well as the usual shear stress considerations. In tension, normal stresses across the particle-matrix interface can cause decohesion of that interface, while in compression decohesion will not occur. Their calculations of the stress field around rigid spherical particles in a homogeneous matrix showed that, in tension, the maximum normal stress on the particle-matrix interface tending to cause decohesion is 1.93 times the applied stress. This stress occurs parallel to the tensile axis. In compression, however, the maximum normal stress on the interface tending to cause decohesion is only 0.21 times the applied stress and occurs normal to the applied stress axis. Since there is a factor of 9 between the normal stress acting upon the interface in tension as compared to compression,

they concluded that for a weak interface it is possible that decohesion can occur in tension at an applied stress below that at which yielding would occur if the interface remained intact. Under a compressive load, however, it is unlikely that interface decohesion would occur before yielding. Yielding in compression then will occur by one of the dislocation-particle interaction mechanisms previously proposed.[10,11,12]

If decohesion does occur, a cavity or void forms at the portion of the particle-matrix interface where the normal tensile stress is greatest. Such cavitation itself would produce an apparent plastic strain that could account for much of the premature yielding in tensile tests. In addition, dislocations will experience a positive (attractive) image force from the part of the interface that has separated, and when dislocations bow between particles they will be partially anihilated at the voids. This means that the residual loop left after bowing is completed will be smaller than the loop left in the case where the interface remains intact. Thus, the decrease in effective interparticle spacing resulting due to the formation of residual dislocation loops will be less in the case where interface decohesion occurs. Assuming that yielding occurs by the bypass of particles by a dislocation bowing mechanism as proposed by Orowan,[10] and that the shear stress required for bowing to occur is proportional to the reciprocal of the mean interparticle spacing, then the yield stress should be lower in the case where decohesion has occurred.

The Olsen-Ansell Model predicts that the SD effect should be observed in dispersion strengthened alloys having a relatively weak particle-matrix interface bond. For stronger interface bonds the magnitude of the SD effect should decrease and eventually disappear for alloys with very strong interfaces.

Olsen, Judd, and Ansell[2] have developed a method to measure this interface strength in TD-Nickel. One of the TD-Nickel alloys they tested exhibited a 30% strength differential, and therefore was expected to have a relatively low interface strength. Since the coefficients of thermal expansion for the metal matrix (nickel[14] $13.5 \times 10^{-6}\ ^{\circ}C^{-1}$) is greater than for the ceramic particles (thoria[15] $9.0 \times 10^{-6}\ ^{\circ}C^{-1}$), they reasoned that if a specimen were heated very rapidly to a high enough temperature, elastic stresses created at the particle-matrix interface would be sufficient to cause dechhesion. By determining this temperature, the stress necessary to cause decohesion could be calculated.

Specimens were heated to a given temperature, and then pulled in tension after holding for some time at temperature. Runs were made for a series of different times at several temperatures, and the yield stress was determined in each case. It was found that, for low temperature, the yield stress was independent of time at temperature. However, for a range of intermediate temperatures the yield strength was found to increase with time at temperature for holding times up to about two seconds. At higher temperatures, the yield strength was independent of time at temperature. The lowest temperature difference (test temperature - room temperature) for which the yield strength was time dependent was used to calculate the interface strength. Actually, this temperature was bracketed and assumed to lie between the highest temperature for which yield strength was time independent and the lowest temperature for which yield strength was time dependent. At this temperature, the yield strength was lowered due to decohesion, but after holding for some time at temperature the voids "healed" (sintered) by diffusion and/or plastic flow restoring the normal yield strength. At lower temperatures there was no decohesion and, therefore, no time dependence of yield strength. At higher temperatures the healing process was apparently fast enough so that the yield strength drop could not be determined.

One purpose of the present investigation was to study the yielding behavior of TD-Nichrome and the relationship of yield strength to the particle-matrix interface strength. Olsen[16] reported an SD effect of 16.5% in one heat of TD-Nichrome. This would predict a higher interface strength than that measured for TD-Nickel.

Tension and compression testing of TD-Nichrome was performed to determine if a strength differential was present and, if so, to what extent. The particle-matrix interface strength was then measured by the method described by Olsen et al,[13] and the relationship of this value to the SD effect was studied. Also, a qualitative comparison of the extent of interface decohesion in TD-Nichrome and TD-Nickel was undertaken by studying the structure of cold rolled specimens using transmission electron microscopy. Scanning electron microscopy studies of high temperature tensile specimen fracture surfaces were used to further investigate the nature of the time dependent yielding phenomenon observed in the measurement of interface strength.

In order to determine the effect of thermal and stress history on the mechanical properties of TD-Nickel and TD-Nichrome, specimens

of these alloys were first exposed to range of superimposed stresses and thermal histories and their room temperature tensile behavior was then determined. This study of the effects of combined stress and thermal cycles was then studied in terms of the thermal fatigue, creep and stress rupture behavior of TD-Nickel at elevated temperatures.

In order to directly determine the stress field developed around the particles in elastically strained two-phase alloys, a tiltable tensile stage was designed for use in transmission electron microscopy studies of the strain constrast developed during the straining of thin foil specimens.

Finally, analytical solutions were calculated of the stress fields developed around dispersed phase particles as the result of external load and differential thermal expansion and the combination of these.

MATERIALS AND APPARATUS

The alloys used in this study were produced commerically by the Fansteel Corporation. TD-Nichrome, consists of a non-coherent dispersion of ThO_2 particles in a matrix of commercial purity 80% nickel - 20% chromium. The particles are spherical with a measured mean particle diameter of 290Å and a mean interparticle spacing of 830Å. The volume fraction of the ThO_2 particles was 2%. Two samples were supplied. The first (heat 3323) was 0.025 inch rolled sheet and was received in the stress-relief annealed condition. The second (heat 3325) was a 0.250 inch rolled sheet, and it was received in the stress-relief only condition, not having been fully annealed.

TD-Nickel, a dispersion of thoria particles in commerically pure nickel, had a mean particle diameter of 400Å and a mean interparticle spacing of 2000Å. The volume fraction of oxide particles was again 2% for this alloy. The sample was received as 0.040 inch sheet in the stress-relief annealed condition.

Tension and compression tests were performed with a Model TT-CM Instron testing machine. For tension tests flexible, self-aligning, wedge-action grips with a load capacity of 20,000 lb. were used with a 5,000 kg. capacity tension load cell. For compression tests a 5,000 kg. compression load cell was used with a special self-aligning table.

Transmission electron microscopy was performed using a Hitachi HU-11B electron microscope. Scanning electron microscopy was performed using a Materials Analysis Corporation Model 400 scanning electron microscope.

Thermal cycling and high temperature load testing was performed using a Duffers Gleeble, Model 501. The Gleeble is capable of resistance heating the specimen at rates up to 15,000°F/sec. and holding the specimen at a constant temperature rate adjustable to a rate as low as 0.01 inches/sec. A 2,000 lb. load cell was used for tensile tests. The temperature, load and elongation were monitored with a Visicorder. By detaching the conventional hydraulic system on this machine and applying dead loads to the specimen grips through a pully arrangement the Gleeble could be used to thermally cycle a preloaded specimens held at a constant load value. This provided a means for using the Gleeble for creep and more complex constant load thermal shock testing. The Gleeble is described in detail by Savage.[18]

METHOD AND PROCEDURE

(1) ROOM TEMPERATURE TENSION AND COMPRESSION TESTING TO DETERMINE MAGNITUDE OF SD-EFFECT IN TD-NICHROME

Room temperature tension and compression tests were conducted on TD-Nichrome to determine if this alloy exhibited an SD effect. Since it was not possible to perform compression tests on the thin sheet of heat 3323 it was necessary to machine specimens from the 0.250 inch plate (heat 3325). Both tension and compression specimens were machined from this heat.

Reduced cylindrical tensile specimens were machined with their axis parallel to the rolling direction. These specimens were 2.5 inches in length and 0.25 inch in diameter with a gauge length of 0.640 ± 0.002 inch and a reduced section 0.160 ± 0.003 inch in diameter. Compression test specimens were also machined with their axis parallel to the rolling direction. They were machined as cylinders 0.25 ± 0.002 inch long and 0.25 inch in diameter. Their ends were ground flat and parallel to within 0.001 inch.

These specimens were annealed for one hour in vacuum at 2400°F to complete the heat treatment prescribe by the Fansteel Corporation. This also served to remove any residual stresses

introduced during the machining operation. Specimens were air cooled from the annealing temperature.

Both compression and tensile specimens were uniaxial loaded at room temperature to determine the 0.2% yield strength. The strain rate used was 0.0026 $sec.^{-1}$ for both tension and compression specimens.

(2) ELECTRON MICROSCOPY OF COLD ROLLED ALLOYS

Several TD-Nickel and TD-Nichrome (heat 3323) specimens were cold rolled to 20%, 40%, 60%, and 80% of the as-received sheet thickness, and the resulting structures were observed in the electron microscope. Specimens were ground to a thickness of approximately 0.006 inch and then 3mm. diameter discs were punched out. These discs were electrochemically polished by a jet polishing technique using the E. A. Fischionne Model 110, twin-jet electropolisher. The electrolyte used was a solution of 20% perchloric acid in ethanol. The polishing voltage was 12 volts.

It should be noted that the structure observed by electron microscopy was not influenced by the grinding or punching operations. Any deformation on the surface of the specimen resulting from grinding was removed by the subsequent electropolishing. The punching was performed in a special jig designed so that only the edges of the disc are deformed, while the center portion which is viewed in the electron microscope was unaffected.

(3) PARTICLE-MATRIX INTERFACE STRENGTH IN TD-NICHROME DETERMINED BY THERMAL SHOCK AND HIGH TEMPERATURE TENSILE TESTING

The method developed by Olsen et al[2] for measuring the particle-matrix interface strength was used in this investigation. TD-Nichrome specimens were made from 0.025 inch sheet (heat 3323). The specimens were 3.0 inches in length, 0.5 inch wide, with a gauge section 1.25 inches long and 0.25 inch wide. A chromel-alumel thermocouple was welded to the middle of each specimen. The Gleeble was programmed to heat the specimen to some temperature between 600°F and 1800°F. The heating rate was the highest obtainable with the Gleeble without producing thermal overshoot. This resulted in rates of 12,000 to 14,000°F/sec. After holding at temperature for a specific time, Δt, the specimens were loaded in tension at an elongation rate of approximately 0.01 in./sec.

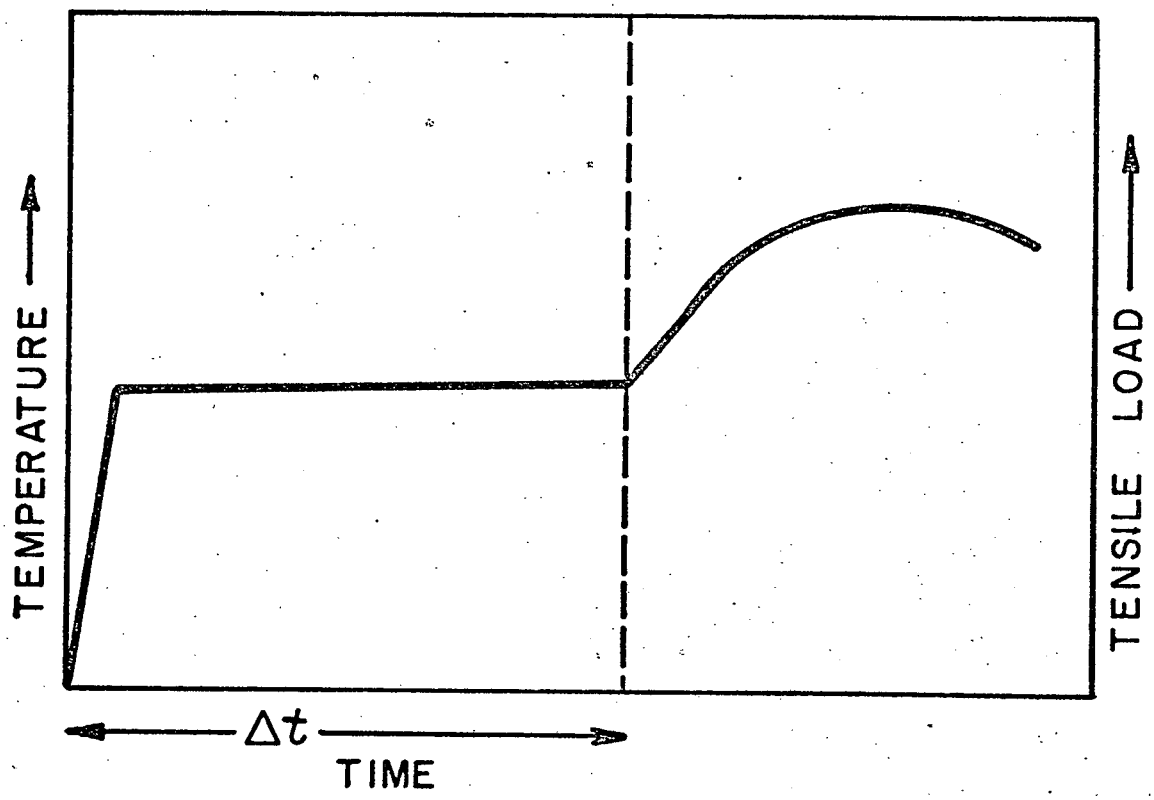

FIGURE 1 GLEEBLE TEST PROGRAM

Although the elongation rate is the same for each specimen, the strain rate cannot be determined exactly since deformation takes place only in that part of the specimen which has reached the maximum temperature. It was assumed that this "hot zone" was 0.5 inch long. The strain rate was thus approximately 0.2 $sec.^{-1}$. Temperature and load are recorded as a function of time. This testing program is illustrated in Figure 1.

(4) SCANNING ELECTRON MICROSCOPY

The time dependence of yield strength at certain temperature indicates that the yielding mechanism may change with time at these temperatures. If this were the case, it was felt that the fracture mode could also be a function of time at temperature. Therefore, the fracture surfaces of several Gleeble specimens were examined with the scanning electron microscope. These represented both long and short times at different temperatures.

(5) EFFECT OF THERMAL CYCLING ON ROOM TEMPERATURE MECHANICAL BEHAVIOR

In order to determine the effect of thermal and stress history on the mechanical behavior of TD-Nickel and TD-Nichrome, specimens of these alloys were first exposed to a range of superimposed stresses and thermal histories and then tension tested at room temperature.

The high temperature portion of the testing was conducted in the Gleeble using a deadloading arrangement to maintain a constant load level on the specimen prior to and during the test cycle. The test specimens were machined from heat 3323 of the TD-Nichrome and from the TD-Nickel in their as received thickness. The specimens were 3.0 inches in length, 0.5 inch wide, with a gauge section 1.25 inches long and 0.25 inch wide. A chromel-alumel thermocouple was welded to the middle of each specimen. The Gleeble was programmed to heat the specimen to the test temperature at a specified rate, held at temperature for a given time, and then to water quench the sample. Specimen loading was accomplished by removing the hydraulic loading arrangement from the specimen grips and replacing the loading device by a dead load attached with flexible wire rope to the grip using a pulley arrangement.

After the high temperature portion of the testing procedure was performed, the specimens were then tested in tension at room temperature in the Instron machine using a strain rate of

$0.0013\ sec.^{-1}$.

Prior to the high temperature and/or room temperature tests, the specimens were annealed either in hydrogen for 1 hour at 1842°F or in argon for 1 hour at 2192°F.

(6) EFFECT OF THERMAL CYCLING ON HIGH TEMPERATURE MECHANICAL BEHAVIOR

In order to test the sensitivity of these alloys to thermal fatigue, specimens of TD-Nickel were preloaded in tension to 24 KSI and then repeatively thermally cycled to 1100°F at two different rates, reaching temperature at two different rates, reaching temperature at either less than 0.25 sec. or in 0.5 sec. The specimen configuration and Gleeble test method used was identical to that used for the previous testing described in (5) preceeding.

In order to determine the effect of combined thermal shock and load on the creep and stress rupture behavior of TD-Nickel, specimens were creep tested at 1100°F as a function of stress and heating rate using the Gleeble. The dead load proceedure was used to stresses of 28 KSI and 29 KSI with the heating rate programmed at either 5,500°F/sec. or 55°F/sec. The specimen configuration was the same as used for the previous tests. Creep deformation was determined during the test by measuring the specimen width during testing with an optical cathetometer rigidly mounted over the center of the gauge section.

(7) DIRECT DETERMINATION OF THE STRESS DISTRIBUTION AROUND HARD PARTICLES IN A STRESSED MATRIX

In order to determine the stress distribution around hard particles in a stressed matrix, the diffraction contrast pattern developed around dispersed phase particles during the elastic straining of two phase alloys in the electron microscope could be utilized. In order to attempt this in this program it was necessary to develop a tensile strain device for the electron microscope which would also allow for changes in specimen orientation during straining in order to permit diffraction analysis. Such a micro-tensile device of this type was designed and constructed in this program to fit within the stereo-hot state of a Hitachi-HU125 electron microscope.

RESULTS AND DISCUSSION

(1) ROOM TEMPERATURE TENSION AND COMPRESSION TESTS

Table 1 shows the results of tension and compression tests on heat 3325 of TD-Nichrome. For these samples there was no significant difference between the tensile and compressive yield strengths. This result was not unexpected since Olsen[16] observed only a small strength differential for this alloy. He also observed that in some heats of TD-Nickel there was no strength differential at all, while others had an SD effect of up to 30%. So, the presence of an SD effect in dispersion strengthened alloys is seen to vary from one heat to another. This variation could be due to changes in chemical composition and/or processing. Olsen[16] showed that small amounts of impurity elements appeared to be associated with the SD effect in TD-Nickel although this effect could not be isolated. However, further work which considers the particle-matrix interface strength in these alloys will most certainly have to include an investigation of the effect of alloying elements on interface strength.

Processing variables may also influence the SD effect. The particular heat tested was supplied as 0.250 inch sheet. Heats tests by Olsen were in the form of 0.250 inch rod. The different processing methods involved could influence the occurrence of an SD effect. Also, this heat was received in the stress relieved condition. The manufacturer specified that a final anneal at 2400°F for two hours was required. This annealing treatment was performed piror to testing. The high yield strengths observed suggest that recrystallization was not complete. To check this several specimens were given additional annealing treatments at 2400°F. The yield strength of these specimens was the same as those previously tested.

These tests show that little or no SD effect is present in TD-Nichrome. This predicts that the interface strength of TD-Nichrome is relatively high. The interface strength must be large enough so that, in tension, decohesion does not occur, before yielding occurs by some other mechanism. The yielding mechanisms in that case should be the same in tension as in compression, and therefore, the yield strength would be expected to be the same in both cases. Other investigations were undertaken to determine the magnitude of the interface strength in TD-Nichrome.

(2) ELECTRON MICROSCOPY OF COLD ROLLED TD-NICKEL AND TD-NICHROME

Figure 2 shows the structure of the as received TD-Nichrome.

TABLE I

RESULTS OF ROOM TEMPERATURE TENSION AND COMPRESSION TESTS

0.2% Yield Strengths

Tension	Compression
102,000 psi	110,000 psi
104,000 psi	105,500 psi
102,000 psi	103,000 psi

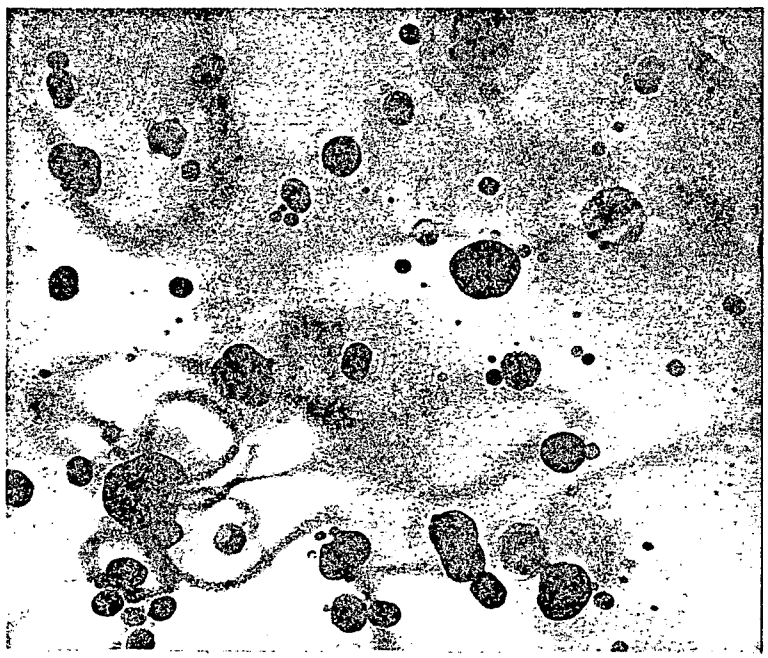

FIGURE 2 AS-RECEIVED TD-NICHROME
(135,000X)

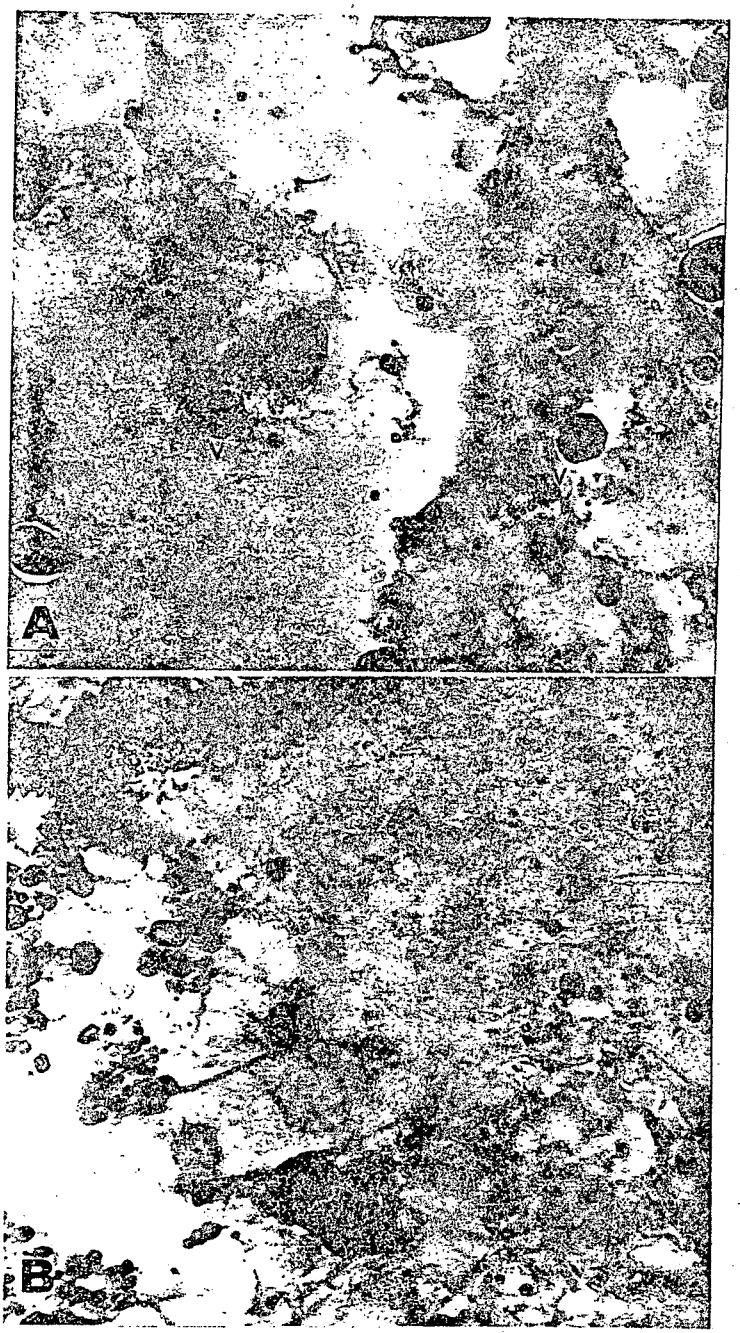

FIGURE 3 (a) TD-NICKEL SHEET, COLD-ROLLED 20%
(b) TD-NICHROME SHEET, COLD-ROLLED 20% (94,000X)

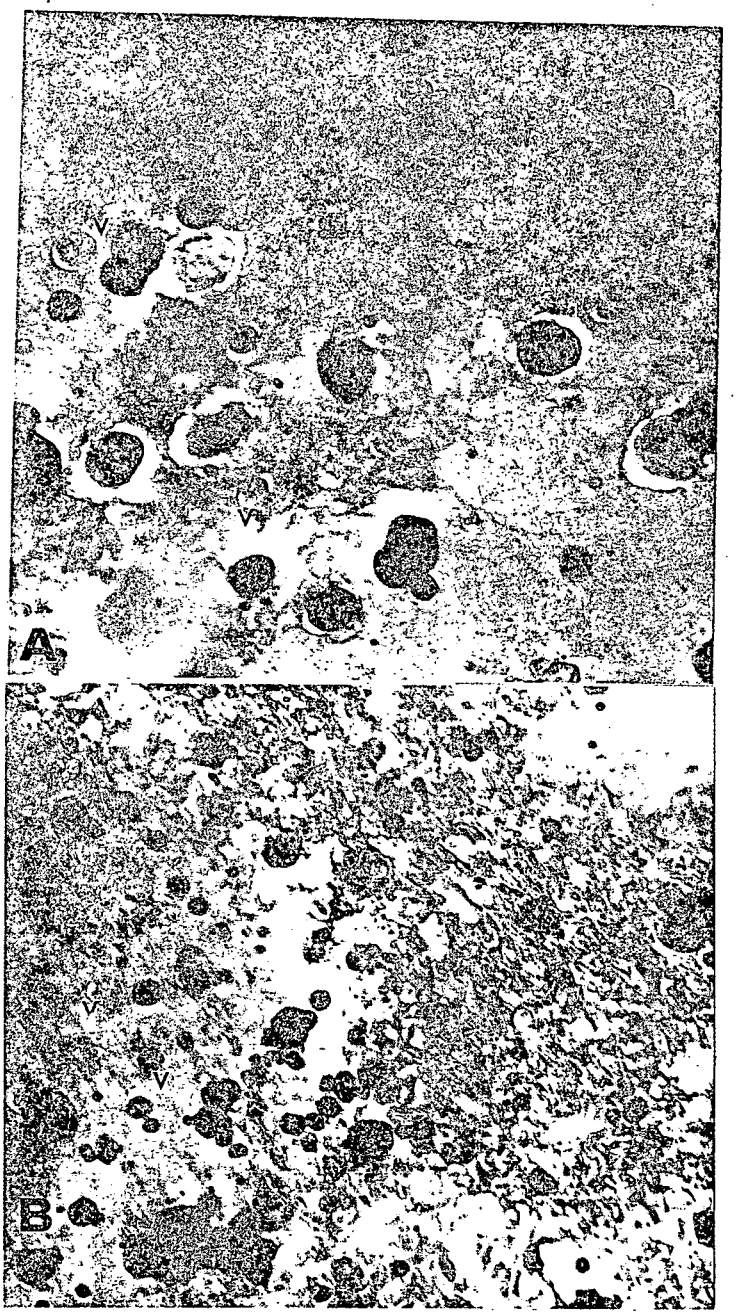

FIGURE 4 (a) TD-NICKEL SHEET, COLD-ROLLED 40%
(b) TD-NICHROME SHEET, COLD-ROLLED 40% (94,000X)

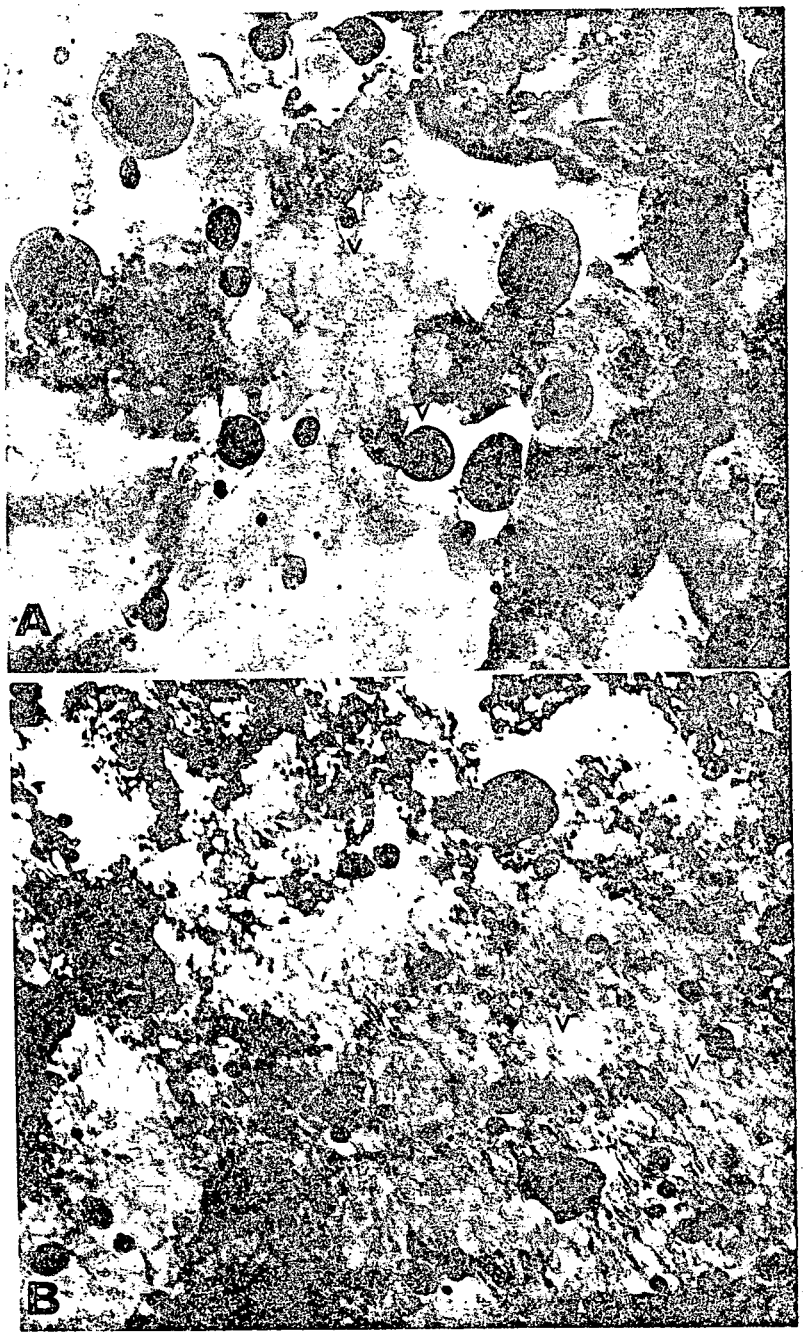

FIGURE 5 (a) TD-NICKEL SHEET, COLD-ROLLED 60%
(b) TD-NICHROME SHEET, COLD-ROLLED 60% (94,000X)

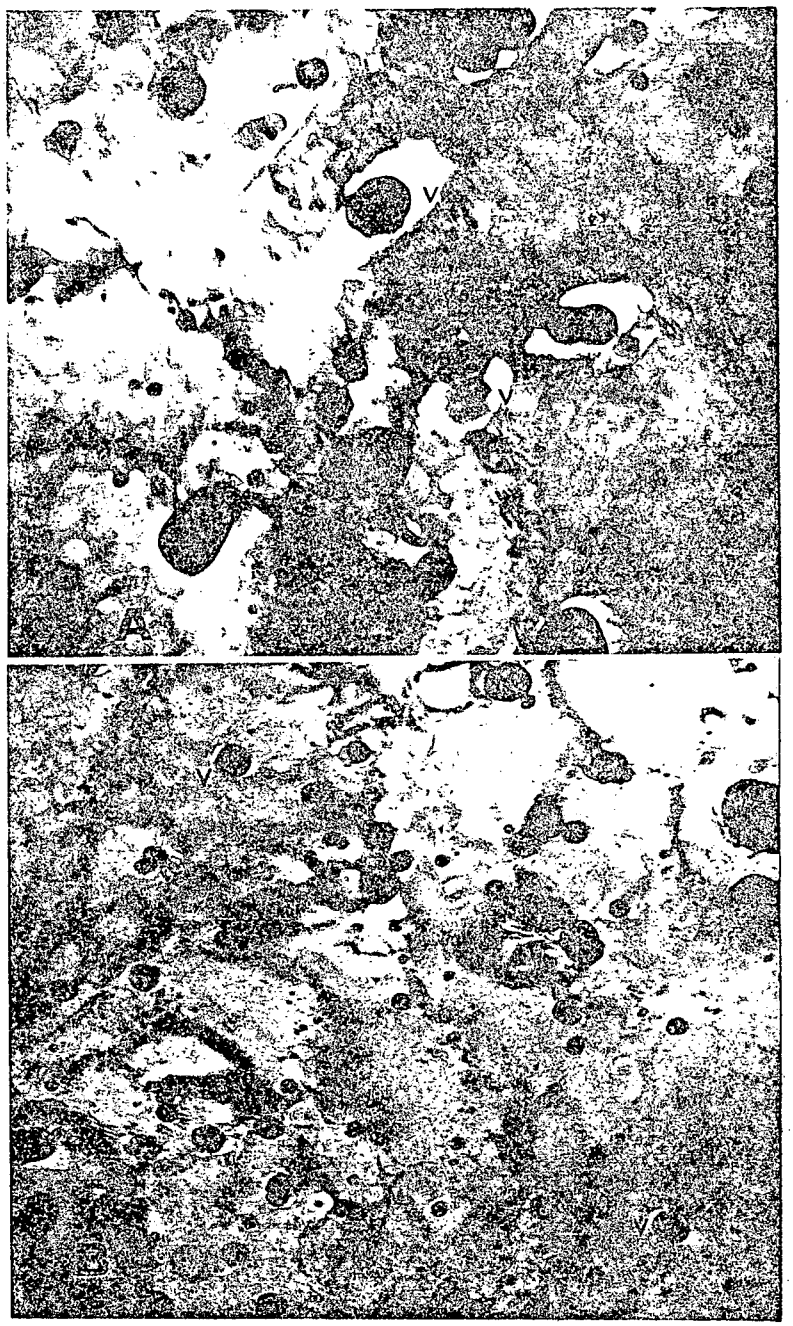

FIGURE 6 (a) TD-NICKEL SHEET, COLD-ROLLED 80%
(b) TD-NICHROME SHEET, COLD-ROLLED 80% (94,000X)

Typical structures resulting from various degrees of cold rolling of TD-Nichrome and TD-Nickel sheet are shown in Figures 3 through 6. Due to the complex nature of the deformation accompanying cold rolling, only a qualitative comparison can be made between the nature of the interface decohesion of these two alloys. One obvious observation is that for large amounts of plastic deformation the interface bond breaks down and void (indicated by "V") form around the particles. These voids are elongated in the direction of rolling. For example, for samples rolled 80% large elongated voids appear in TD-Nickel. TD-Nichrome also exhibits voids at the particles after 80% rolling. However, fewer particles appear to have voids associated with them. Also, the voids are not as elongated as in TD-Nickel.

This trend continues down through lesser amounts of rolling. At 40% and 20% rolling TD-Nickel still has voids associated with most of the particles, while in TD-Nichrome relatively few particles have voids.

The fact that voids from after extensive plastic deformation in both these alloys is not surprising. Olsen and Ansell[1] reported that cold rolling separated the particle-matrix interface in TD-Nickel. They also showed that a similar void structure resulted when specimens were plastically deformed in a tensile test. Palmer and Smith[19] showed similar formations in internally oxidized Cu-Si and Cu-Be alloys after 20% elongation. Webster[20] developed a model for this type of deformation proposing that it was common to system consisting of hard spherical particles in a ductile matrix.

However, this type of void formation has most often been associated with relatively large amounts of plastic deformation or with fracture. Indeed, void nucleation at particles followed by void coalescence is commonly accepted as the fracture mechanism in dispersion strengthened alloys.[21] Olsen and Ansell,[1] however, proposed that particle-matrix decohesion and subsequent void formation could take place at lower strains as a result of elastically induced stresses and, as a result cause macroscopic yielding. For very small amounts of plastic deformation, then, voids should be present although they will be so small that they will not be observable by electron microscopy. For instance, Olsen et al[2] calculated that an apparent strain of 0.0015 would be produced in TD-Nickel by the formation of voids with a mean width of 10Å. In this case a significant amount of strain is present due to voids which are not resolvable.

Figure 3 through 6, are not intended to associate void formation with yielding. They do point out that void formation is more prominent in TD-Nickel than in TD-Nichrome. This could indicate that interface failure occurs at a lower stress in TD-Nickel than in TD-Nichrome resulting in more extensive void formation in the TD-Nickel, especially at small amounts of deformation. If the TD-Nichrome does indeed have a stronger particle-matrix interface bond, then it would be expected that the SD effect in TD-Nichrome would be less than in TD-Nickel if it appeared at all. This is consistent with the data obtained from mechanical tests on TD-Nichrome both in this investigation and by Olsen.[16]

However, it could be argued that interface fracture is occurring in TD-Nichrome at low stresses, but that decohesion is not as prominent as in TD-Nickel because voids do not grow as readily. This could be a result of the greater inherent strength of the Nichrome matrix which would inhibit the growth of voids. Therefore, these results are not conclusive in demonstrating that the particle-matrix interface bond in TD-Nichrome is stronger than that in TD-Nickel, and it was necessary to perform further tests to obtain quantitative results.

(3) THERMAL CYCLING AND HIGH TEMPERATURE TENSILE TESTING

Specimens were tested after holding at 650°, 1200°, 1500°, and 1800°F for various times following rapid heating to temperature. The 0.2% yield strength was measured for each specimen. Yield strength as a function of time at temperature (Δ t) is plotted in Figure 7 for the four temperatures used in this investigation. For the three lower temperatures there appears to be no variation of yield strength with time at temperature. At 1800°F, however, yield strength increases from about 25,000 psi at 0.4 seconds to 32,000 psi for times of 5 seconds or more. This represents about a 22% decrease in yield strength for short times as compared to long times at temperature.

Therefore, at some temperature between 1500° and 1800°F a transition occurs. Above this temperature the yield strength becomes time dependent up to about 5 seconds. For longer times at 1800°F the yield strength is again time independent. At the 1800°F level itself, then, there is a transition from time dependent yielding to time independent yielding. At temperatures below the transition temperature yield strength is time independent.

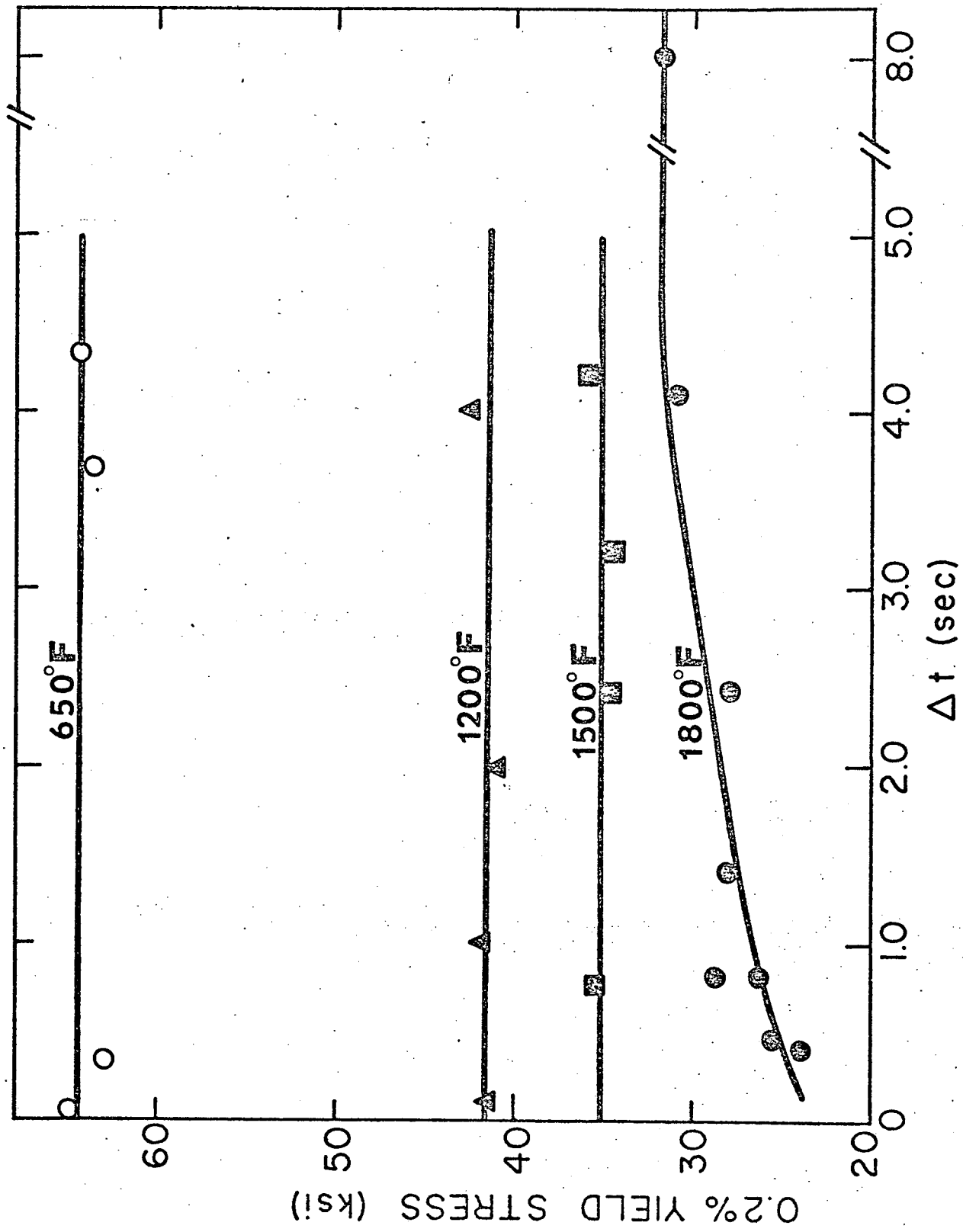

FIGURE 7 YIELD STRENGTH OF TD-NICHROME AS A FUNCTION OF TIME AT TEMPERATURE

The transition from time independent to time dependent yielding with increasing temperature is thought to be a result of particle-matrix interface decohesion due to differential thermal expansion stresses. Olsen et al[2] observed that this transition occurred in TD-Nickel at about 590° to 650°F. TD-Nichrome exhibits a considerably higher transition temperature. Below the transition temperature the differential thermal expansion stresses produced by rapid heating are not high enough to break the particle-matrix bond. Above this temperature, however, these stresses are higher, and voids nucleate at the particle-matrix interface. The presence of these voids results in an anomalously low yield strength if the sample is tested immediately after heating. The transition temperature is then the temperature which produces differential thermal expansion stresses which are just high enough to cause decohesion of the particle-matrix interface.

The differential thermal expansion stress on the interface at this temperature is representative of the interface strength. The interface strength is given by the equation: due to Rao et al[13].

$$\sigma_i = \frac{-6 E_m K_p}{2E_m + 3K_p (1 + \nu_m)} \left(\frac{1 + \alpha_p \Delta T}{1 + \alpha_m \Delta T} - 1 \right)$$

For the nichrome-thoria system the terms of this equation have the following values:

$$E_p = 37.8 \times 10^6 \text{ psi}^{22}$$

$$E_m = 31.0 \times 10^6 \text{ psi}^{17}$$

$$\nu_p = 0.275^{23}$$

$$\nu_m = 0.30 \text{ (approx.)}$$

$$K_p = \frac{E_p}{3 (1 - 2 \nu_p)} = 28.0 \times 10^6 \text{ psi}$$

$$\alpha_m = 17.3 \times 10^{-6} \text{ °C-1}$$

$$\alpha_p = 9.0 \times 10^{-6} \text{ °C-1}$$

ΔT is the increase in temperature from room temperature (70°F) to the transition temperature which is between 1500°F and 1800°F.

For 1500°F, $\Delta T = 1500 - 70 = 1430°F = 795°C$

$$\sigma_i = 198{,}000 \text{ psi}$$

For 1800°F, $\Delta T = 1800 - 70 = 1730°F = 960°C$

$$\sigma_i = 238{,}000 \text{psi}$$

Therefore an estimate of the interface strength is between 143,000 psi and 172,000 psi. These values are considerably higher than the interface strength measured by Olsen *et al*[2] for TD-Nickel. They obtained an average value of 31,000 psi.

For TD-Nichrome, then, it is much less likely that interface decohesion will occur prior to yielding. The stronger interface bond in this alloy is consistent with the fact that little or no SD effect is observed.

It is important to note that the interface strength was measured for heat 3323 (0.025 inch sheet) while tension and compression data was obtained from heat 3325 (0.25 inch plate). Therefore, since wide variations in mechanical behavior have been observed from heat to heat in these alloys, it is not possible to derive any quantitative relationship between the interface strength and the magnitude of the SD effect. However, it is possible to conclude that the interface strength is TD-Nichrome is signicantly greater than that in TD-Nickel. As measured by this technique, the TD-Nichrome particle-matrix interface strength was about five times greater than that measured by Olsen *et al*[2] for TD-Nickel.

At 1800°F the yield strength increases with time up to about 5 seconds. For longer times it remains constant. This behavior was also observed by Olsen *et al*[2] in TD-Nickel, but they found that for higher temperatures (1800°F in that case) the time dependence disappeared. They hypothesized that voids formed during up-quenching healed with time at temperature, and after a few seconds the yield strength returned to its normal value. Indeed, the detection of a critical temperature to cause interface decohesion is dependent on this healing process, which produces a change in yield strength with time. Olsen *et al*[2] reported that the yield strength of TD-Nickel returned to its normal value after about 2 seconds at 1100°F, while at 1800°F healing of voids occurred so rapidly that no time dependence could be detected. TD-Nichrome, on the other hand, did not fully recover for 4 or 5 seconds at 1800°F. This recovery time is related to the kinetics of the process by which healing of the voids occurs and is not well understood at this time. It is believe that plastic flow

and/or diffusion mechanisms could be operating to cause healing of voids, and in this sense the phenomenon is similar to a sintering mechanism.

The fact that the healing process is slower in TD-Nichrome than in TD-Nickel is an interesting result in itself. If diffusion was the controlling mechanism it would be unlikely that such a long recovery time would be observed at 1800°F for TD-Nichrome, while recovery was instantaneous in TD-Nickel. However, if plastic flow were the healing mechanism it is quite likely that the nickel matrix would heal more rapidly than the nichrome matrix. The solid solution strengthening effect in nichrome would act as a barrier to plastic flow, and thus slow down the healing process. Therefore, while this data is in no way meant to be conclusive evidence, it does point out that plastic flow is a more credible mechanism to explain the healing process.

(4) SCANNING ELECTRON MICROSCOPY OF HIGH TEMPERATURE TENSILE SPECIMEN FRACTURE SURFACES

The fracture surface of several room temperature and high temperature tensile specimens were examined with the scanning electron microscope. It was believe that if the yielding mechanism were time dependent then this dependence might also be observed in the fracture mode. That is, if voids were open during yielding after short times at temperature, then the applied stress should be sufficient to hold them open up to the time of fracture. However, if voids were not open at yielding then the fracture surface would not show evidence of void formation, unless voids opened during plastic deformation. Although it is known that voids will nucleate during plastic deformation at room temperature, it is not necessarily true that this mechanism occurs at high temperatures.

Figure 8 shows the appearance of the TD-Nichrome tensile specimen fracture surface at room temperature. Its appearance is typical of dispersion strengthened alloys.[21] The surface has a dimpled texture which is associated with ductile failure by void coalescence and growth. The dimples are extremely small, indicating that voids were nucleated on many sites. This correlates with the fact that voids nucleate at the particle-matrix interface, so that every particle is a potential nucleation site for a void and subsequent dimple formation.

Scanning electron micrographs of high temperature tensile specimen fracture surfaces are shown in Figure 9 through 11, for tests conducted at 1200°F and 1500°F there was no time dependence of the yield stress. Figure 9 shows that the appearance of the fracture surface does not change as a function of time at 1200°F. Figure 10 shows that there is also no change at 1500°F. In both cases the fracture surfaces have the typical dimpled appearance similar to that observed in room temperature tensile specimens. Fracture then is occurring by a similar mechanism. Dimples in the high temperature samples appear to be larger than those in the room temperature samples. This is most likely due to the relative ease of plastic deformation at high temperatures allowing void growth and coalescence to occur. At low temperatures void growth is more difficult so more fine voids will appear on the fracture surface.

At 1800°F the appearance of the fracture surface changes significantly. Figure 11b shows the fracture surface of a specimen pulled to fracture after 4.2 seconds at 1800°F. In this sample and in other held for several seconds at 1800°F fracture appears to have occurred by an intergranular mechanism. The macroscopic appearance of these surfaces was very rough and faceted. Figure 11b shows one of these large facets. The fracture mode in this case appears to be intergranular. Individual grains of TD-Nichrome can be seen in the scanning electron micrograph. Some of the larger oxide particles also appear. This fracture surface indicates that voids at oxide particles did not form in this sample even after large amounts of plastic deformation.

Figure 11a is a fracture surface of a specimen pulled to fracture after 0.8 seconds at 1800°F. This surface also was roughly faceted on a macroscopic level having about the same appearance as the sample tested after 4.2 seconds at 1800°F. However, in Figure 11a it can be seen that the microscopic appearance is quite different. The facets appear to be rounded, and within the facets the surface is marked by many cavities. In some of the surface cavities oxide particles are visible. There is then a time dependence of the fracture surface appearance at 1800°F which corresponds to the time dependence of yield strength.

The mechanism proposed to explain the yield strength time dependence could also be applied to the fracture surface. When TD-Nichrome is heated rapidly to 1800°F the difference in thermal expansion is enough to cause particle-matrix decohesion. If the

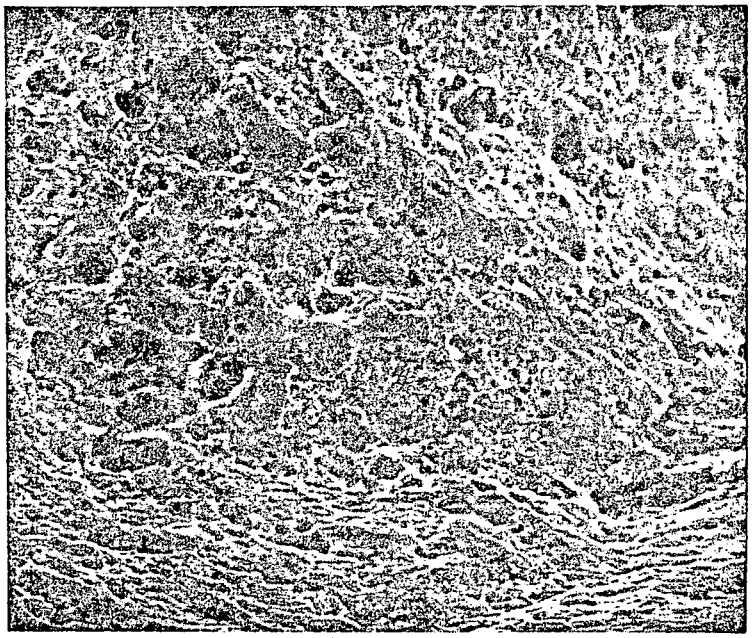

FIGURE 8 FRACTURE SURFACE OF TD-NICHROME ROOM TEMPERATURE TENSILE SPECIMEN (2,000X)

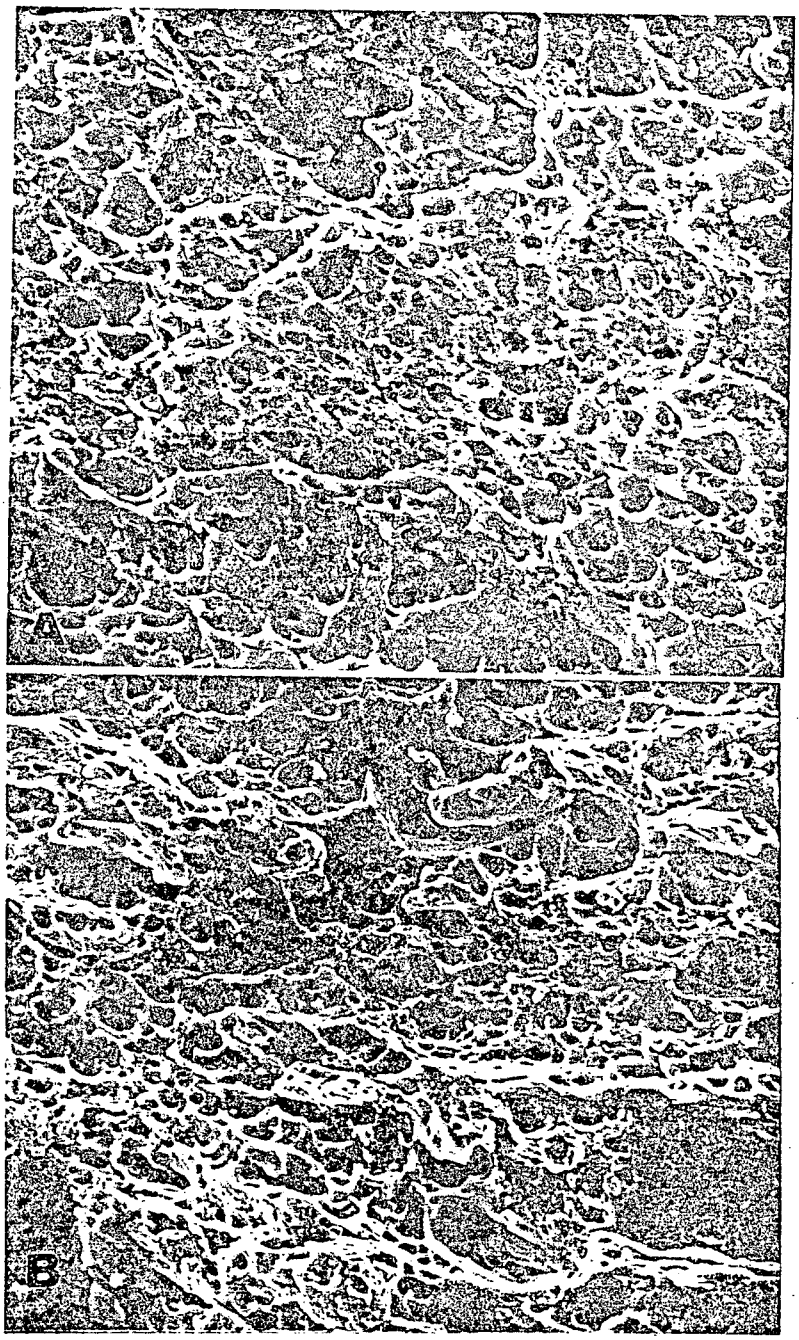

FIGURE 9 FRACTURE SURFACES OF TD-NICHROME TENSILE SPECIMENS PULLED TO FRACTURE AFTER
(a) 0.1 SECONDS AT 1200°F,
(b) 4.0 SECONDS AT 1200°F.
(2,000X)

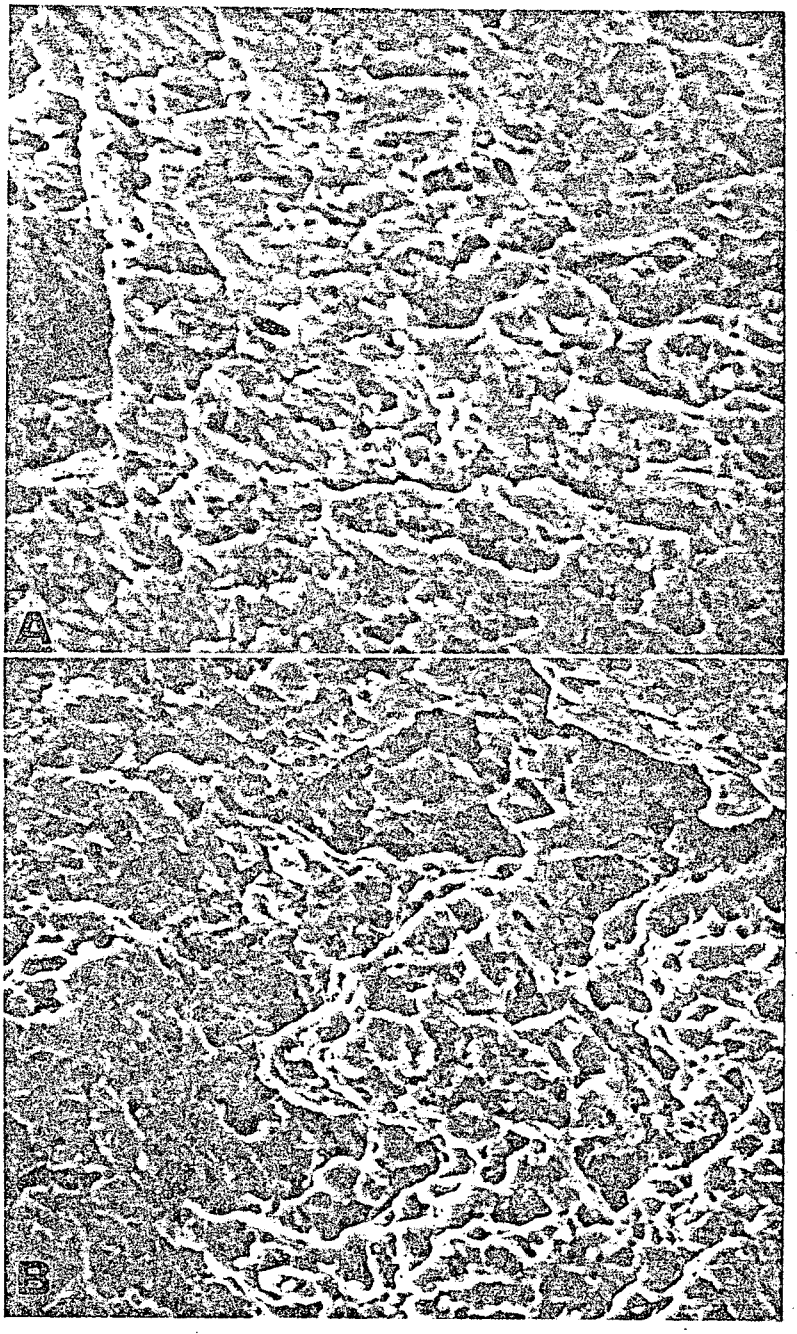

FIGURE 10 FRACTURE SURFACES OF TD-NICHROME TENSILE SPECIMENS PULLED TO FRACTURE AFTER
(a) 0.75 SECONDS AT 1500°F,
(b) 3.2 SECONDS AT 1500°F.
(2,000X)

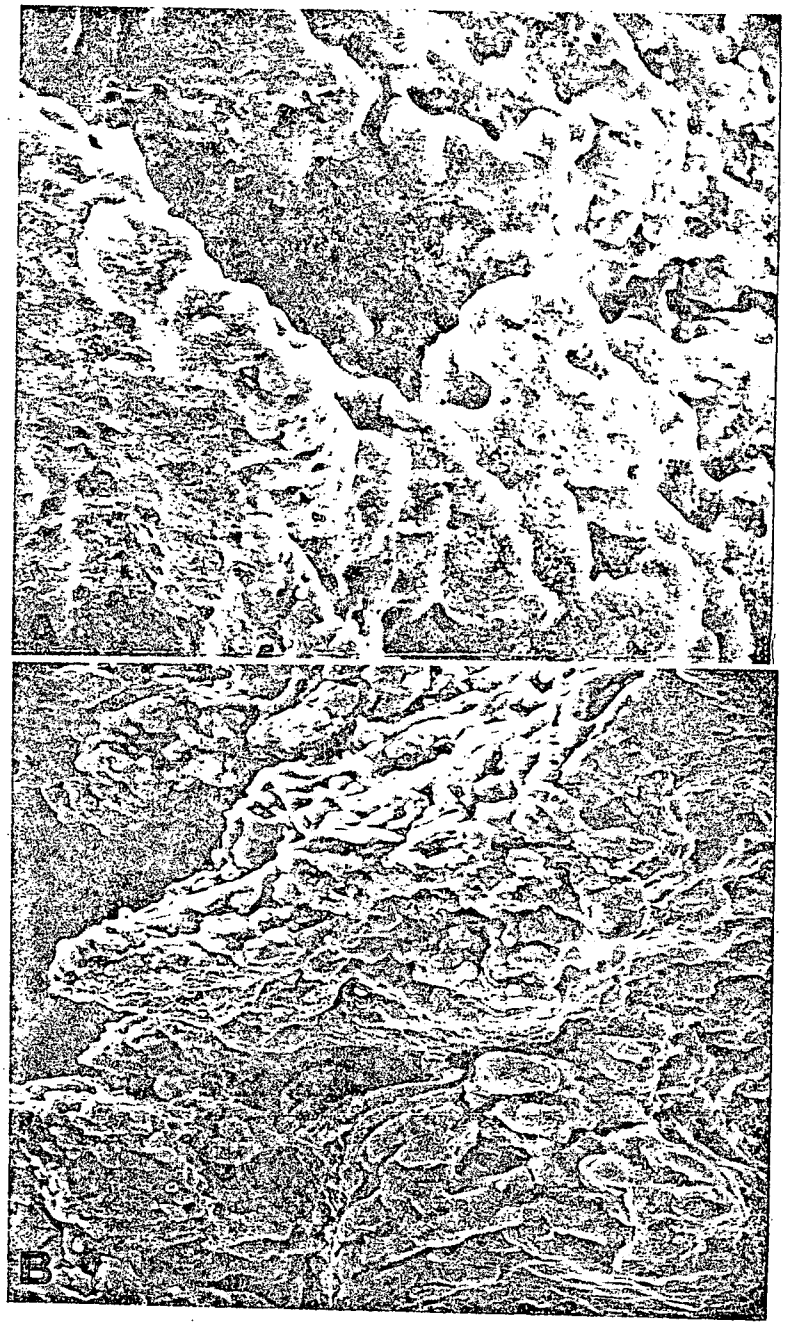

FIGURE 11 FRACTURE SURFACE OF TD-NICHROME TENSILE SPECIMENS PULLED TO FRACTURE AFTER
(a) 0.8 SECONDS AT 1800°F,
(b) 4.2 SECONDS AT 1800°F.
(2,000X)

specimen is tensile tested immediately the applied stress will open voids around particles where the interface has separated. These voids will grow until gross fracture occurs and, therefore, should appear on the fracture surface. It is believed that the small holes on facets of the fracture surface in Figure 11a are caused by this kind of mechanism. The apparent presence of small particles in some of the holes support this theory. It should be noted that fracture in this case does not appear to occur by void coalescence as in the lower temperature tensile specimens. The fracture surface does not have the normal dimpled appearance. Instead fracture is believed to occur intergranularly.

For samples held for longer times at 1800°F the particle-matrix interface heals. When stress is applied the weakest part of the structure is the grain boundaries, and deformation occur here resulting in intergranular fracture. Stress on the particle-matrix interface does not reach a high enough value to cause decohesion, and there is no evidence of void formation on the fracture surface. Therefore, it appears that at 1800°F fracture occurs intergranularly, but the fracture surfaces of samples tested after long and short times are markedly different.

The importance of this evidence lies in the fact that it shows that voids are actually formed by differential thermal expansion during very fast heating to a sufficiently high temperature. This supports the validity of using the method developed by Olsen et al of up-quenching followed by high temperature tensile testing in the Gleeble to determine the particle-matrix interface strength in dispersion strengthened alloys. It also supports the theory that voids heal if the specimen is allowed to remain unstressed at temperature for a sufficient length of time.

The one result that is not fully understood is the rounded appearance of the facets on the fracture surface of the short time, 1800°F sample (Figure 11a). This appearance suggests that some melting has occurred on the fracture surface. This is most likely a result of local temperature fluctuations immediately prior to fracture. As the sample begins to fracture, that area which has not yet fractured will experience a very high current density and therefore a sharp rise in temperature. This could result in localized melting which would explain the rounded appearance of the fracture surface. However, this melting does not appear to influence the formation of cavities on the surface.

Figure 12 shows a specimen tested after 4.2 seconds at 1800°F which also exhibited this type of rounding off on the facets of the fracture surface. However, this specimen does not exhibit the cavities seen in Figure 11a. Therefore, it is feld that the cavities form as a result of the up-quench and are not an artifact resulting from localized melting of the fracture surface.

(5) EFFECT OF THERMAL CYCLING ON ROOM TEMPERATURE MECHANICAL BEHAVIOR

In order to determine the effect of thermal history on the mechanical behavior of these alloys specimens of TD-Nichrome (heat no. 3323) and TD-Nickel were first exposed to a range of superimposed stress and thermal histories and then tensioned tested at room temperature. The room temperature tests were performed in the Instron machine using a strain rate of 0.00128 $sec.^{-1}$. The sheet gleeble specimen geometry was used for all tests. The specific thermal and stress histories for each test and the resultant room temperature strengths determined are showm in Table II.

These results indicate the following. The room temperature yield strength of the TD-Nickel specimens drop after 1 hour anneals at 1842°F and 2192°F, the later being more significant. The lower temperature anneal is prcbably tied to stress relief and the higher temperature anneal tied to some operative recovery mode. Thermal cycling to 1150°F, with and without dead load, in the stress, time and temperature range where void initiation should occur had no significant effect on the room temperature tensile properties.

The results for the TD-Nicrome specimens contrast with those for the TD-Nickel. Here, the high temperature anneal minimized the scatter in the room temperature yield strength, probably as a result of stress relief, but did not alter the yield strength. The first set of thermal cycles carried out without load were programmed not to produce voids, but rather to use the hold time at temperature to sinter them shut. In this way the differential thermal expansion between the thoria particles and the matrix can be used to deform the specimen. This thermal cycle reduced the room temperature yield strength probably as a result of a dynamic recovery process. The last set of specimens, those preloaded to 19.2 KSI, were held at temperature for only 0.1 sec. Here, the preload and short hold time at temperature were chosen to keep the voids open. These specimens had a

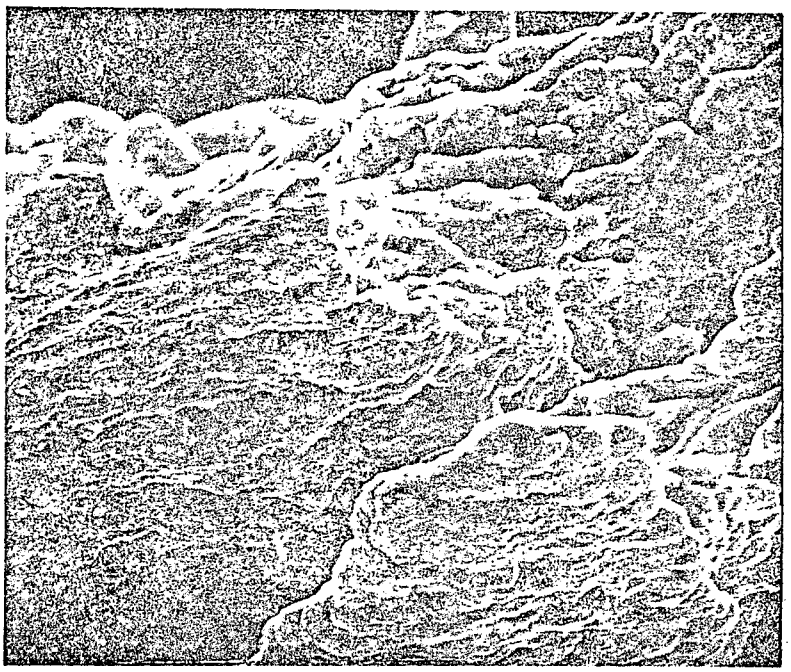

FIGURE 12 FRACTURE SURFACE OF TD-NICHROME TENSILE SPECIMEN PULLED TO FRACTURE AFTER 4.2 SECONDS AT 1800°F (2,000X)

TABLE II

Alloy	Thermal and Stress History	0.2% Offset Yield Strength (KSI)
TD-Nickel	as received and machined	49.5 41.0 45.0
TD-Nickel	annealed in H_2 for 1 hr at 1842°F	41.0 39.0 36.0 42.0
TD-Nickel	annealed in Argon for 1 hr at 2192°F	35.0 36.0
TD-Nickel	annealed in Argon for 1 hr and then heated to 1150°F in 0.1 sec., held at temperature for 0.1 sec., and then water quenched to room temperature in 0.1 sec. During the thermal cycling the specimens were dead loaded to the specified stress P.	38.0 (P = 0) 34.0 (P = 6 KSI) 34.5 (P = 6 KSI) 40.0 (P = 10 KSI) 39.0 (P = 10 KSI) 40.0 (P = 12 KSI) 36.0 (P = 12 KSI) 38.0 (P = 14 KSI)
TD-Nichrome	as received and machined	76.8 84.4
TD-Nichrome	annealed in Argon for 1 hr at 2192°F	80.0 81.5
TD-Nichrome	annealed in Argon for 1 hr and then thermally cycled without load using the following thermal cycle. Heated to 1800°F in 0.3 sec., held 10 sec. at temperature, and then water quenched to room temperature in 0.1 sec. The samples were held 8 sec. at room temperature between each thermal cycle.	73.5 (5 cycles) 75.2 (5 cycles) 73.6 (10 cycles)

TABLE II (Continued)

Alloy	Thermal and Stress History	0.2% Offset Yield Strength (SKI)
TD-Nichrome	annealed in Argon for 1 hr and then thermally cycled once to 1800°F while dead loaded to 19.2 KSI. The thermal used was heating to 1800°F in 0.3 sec., held 0.1 sec. at temperature, and then water quenched to room temperature in 0.1 sec.	55.0 72.7 65.6 63.2

significant drop in room temperature yield strength in contrast to the results obtained for the TD-Nickel.

In order to further explore the effects of combined thermal stress with superimposed loading a sequence of tests were undertaken to examine the room temperature stress-strain behavior of TD-Nickel after prior exposure to a range of superimposed stressed and thermal histories. All specimens were heated to 1100°F in 0.1 sec., held at temperature for 0.1 sec. and then water quenched to room temperature in 0.1 sec. During the thermal cycle, the specimens were preloaded using stresses of 2, 4, 6, 8, 10, 14 and 16 KSI. After cooling the room temperature stress-strain behavior was determined. The results obtained are shown in Fig. 13. All of the test data lie in the shaded region of the tensile curve. There doesn't appear to be any effect of the preload stress on the resulted behavior. On this basis it appears that this range of prior thermal shock and load history has little effect on the room temperature tensile behavior of TD-Nickel. This is somewhat surprising in view of its effect on high temperature properties.

(6) EFFECT OF THERMAL CYCLING ON HIGH TEMPERATURE MECHANICAL BEHAVIOR

Specimens of TD-Nickel were perloaded to 24,000 psi in tension and then rapidly thermally cycled to 100°F. (The 1100°F yield strength is 30 KSI.) Those specimens which were heated to 1000°F is less than 0.1 sec., reaching 1100°F in less than 0.25 sec., fractured after 19 to 25 cycles. Similarly loaded specimens, heated more slowly, reaching 1100°F in 0.5 sec., did not fracture after 100 thermal cycles.

In order to determine whether sequential rapid thermal cycling might alter the grain shape and size in these alloys in addition to its effect in producing interface decohesion, samples of as received TD-Nickel sheet were compared metallographically with equivalent samples which had been cycled 15 times from room temperature to 1100°F in times of less than 0.2 sec. Metallographic examination showed no difference between the grain shape and size in the cycled and uncycled materials.

These data were there interpreted in terms of the stress generated by the differential thermal expansion between the thoria

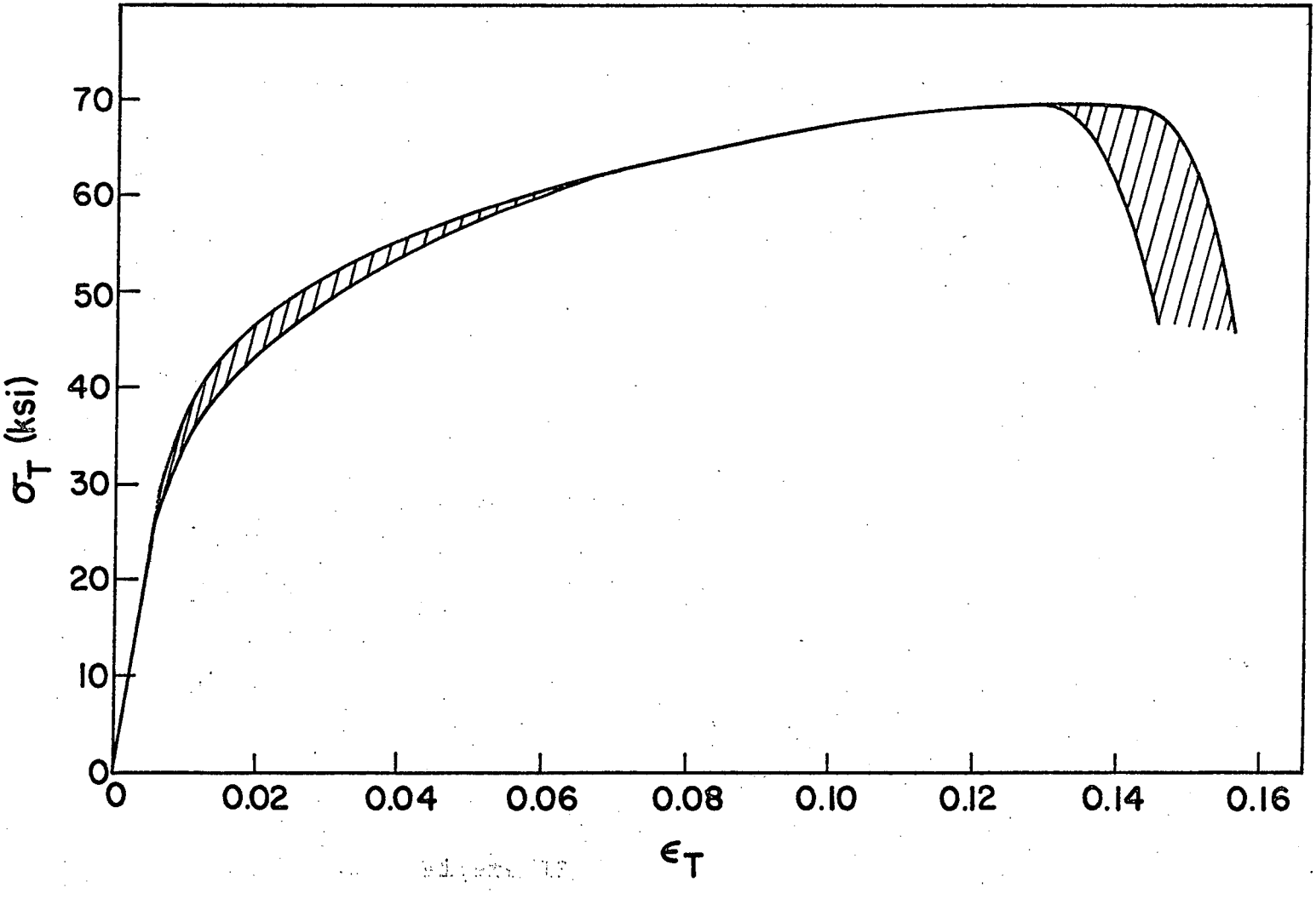
70
60
50
40
30
20
10
0
σ_T (ksi)
0
0.02
0.04
0.06
0.08
0.10
0.12
0.14
0.16
ϵ_T

Figure 13

particle and nickel matrix causing particle-matrix interface failure, hence weakening the thermally shocked samples. In order to persue this behavior, creep and stress rupture studies of similarly exposed specimens were undertaken.

Specimens of TD-Nickel were tested creep tested at 1100°F as function of tensile load and the heating rate used to reach test temperature. Specimens were preloaded at room temperature to the test stress and then heated to 1100°F in either 0.2 sec. (5,500°F/sec.) or 20 sec. (55°F/sec.) and their minimum creep rates and stress rupture lives determined. Stresses of 28 KSI and 29 KSI were used and the results obtained are shown in Fig. 14.

The results of these experiments show the following behavior. First, at both stress levels, the stress rupture life is significantly reduced with the 5,500°F/sec. heating rate. For the 29 KSI data, the stress rupture life at 55°F/sec. was 17½ hours as compared to 5½ hours for the 5,500°F/sec. heating rate. For the 28 KSI data, the stress rupture life decreased from more than 25 hours at 55°F/sec. as compared with 10½ hours for the 5,500°F/sec. heating rate. Second, the minimum creep rate obtained for the specimens heated at the foster rate were significantly higher than for those heated at 55°F/sec. At 29 KSI, the minimum creep rates were $1.06 \times 10^{-6} min^{-1}$ for the 5,500°F/sec. heating rate as compared to $2.57 \times 10^{-7} min^{-1}$ for the 55°F/sec. heating rate. At 28 KSI the minimum creep rates were 2.47×10^{-7} min^{-1} for 5,500°F/sec. heating rate as compared to 1×10^{-7} min^{-1} for the 55°F/sec heating rate. Third, the stress dependence of the minimum creep rate appears to be sensitive to the initial heating rate. The steady-state creep rate of dispersion strengthened alloys, including TD-Nickel, generally is observed to follow an exponential dependence on stress of the form, at constant temperature, $\dot{\epsilon} = K\sigma^n$ where $\dot{\epsilon}$ is the steady-state creep rate, σ is the applied stress, K is a proportionality constant and n is the stress exponent. These data indicate that n increases from 27 for the specimens heated at 55°F/sec. to 43 for the specimens heated at 5,500°F/sec. One notes that more data is required to accurately determine the exact values of n as well as the characteristic steady-state creep rates and stress-rupture lives. However, these results strongly indicate the substantial effect that the prior heating rate has on the high temperature behavior of this alloy.

These results can be interpreted in terms of the generation of tensile stresses at the dispersed thoria particle to nickel

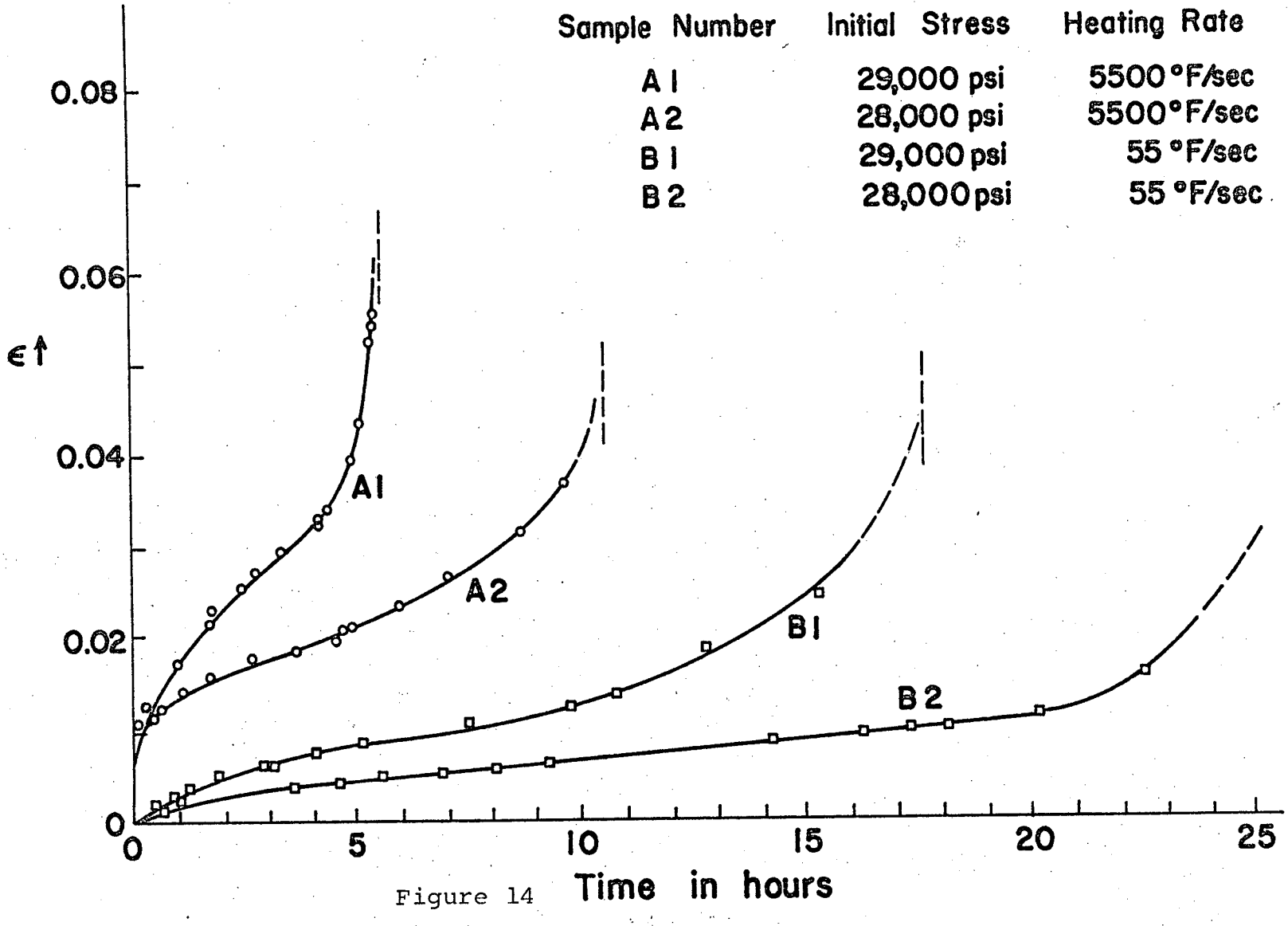
Sample Number
Initial Stress
Heating Rate
A 1
29,000 psi
5500°F/sec
A 2
28,000 psi
5500°F/sec
B 1
29,000 psi
55 °F/sec
B 2
28,000 psi
55 °F/sec
0.08
0.06
0.04
0.02
0
ε↑
A1
A2
B1
B2
0
5
10
15
20
25
Time in hours

Figure 14

matrix leading, in the case of rapid heating, to interface rupture. Slow heating allows stress relaxation to occur during the heating cycle, reducing the possibility of interface rupture. In order to determine the plausibility of this argument, structural studies of the crept specimens were directed towards the detection of these voids. To this end, samples were creep tested at the same stress, temperature and heating rate used previously to 1% strain. After 1% strain, the specimens were water quenched and a ½ inch length from the center of the gauge length removed. Precision density measurements were made of these samples as a means of determining interface failure and pore generation. For the density measurements, specimens were first polished to remove oxide from the surface and then suspended in a copper wire basket, and weighed first in air and then in carbon tetrachloride using a mettler analytical balance. The temperature of the carbon tetrachloride was measured before and after each weighing to enable the use of the appropriate density value of carbon tetrachloride in the calculations. Care was taken to immerse the wire to the same depth in the liquid each time.

The mean value, standard deviation, and 95% confidence band were calculated for each of the two sets of specimens. The set of specimens heated slowly to temperature exhibited a density of 8.931 ± 0.007 gms/c.c. (applying 95% confidence limits) while the set heated rapidly to creep temperature had a density of 8.926 ± 0.005 gms/c.c. While not definitive, the slightly smaller mean density for the rapidly heated specimens is probably due to microvoid formation.

(7) DIRECT DETERMINATION OF THE STRESS DISTRIBUTION AROUND HARD PARTICLES IN A STRAINED MATRIX

The micro-tensile strain device, shown in Fig. 15, was designed and constructed during this program. The device was capable of providing steoscopic motion and controllable strain to the sample by remote operation with good sensitivity and response. As in some previous devices, strain is imposed on the sample mounted between two bimetallic strips by symmetric deflection of the simultaneously heated strips. The bimetallic strips, mounted on a stretching cartridge, are heated by teflon-coated nichrome winding wound in series on the strips with a total resistance of approximately 20 ohms. The strips are 0.025 inch thick and are made of proprietory Fe-Ni thermal expansion alloys differing in composition. The stretching and bottom

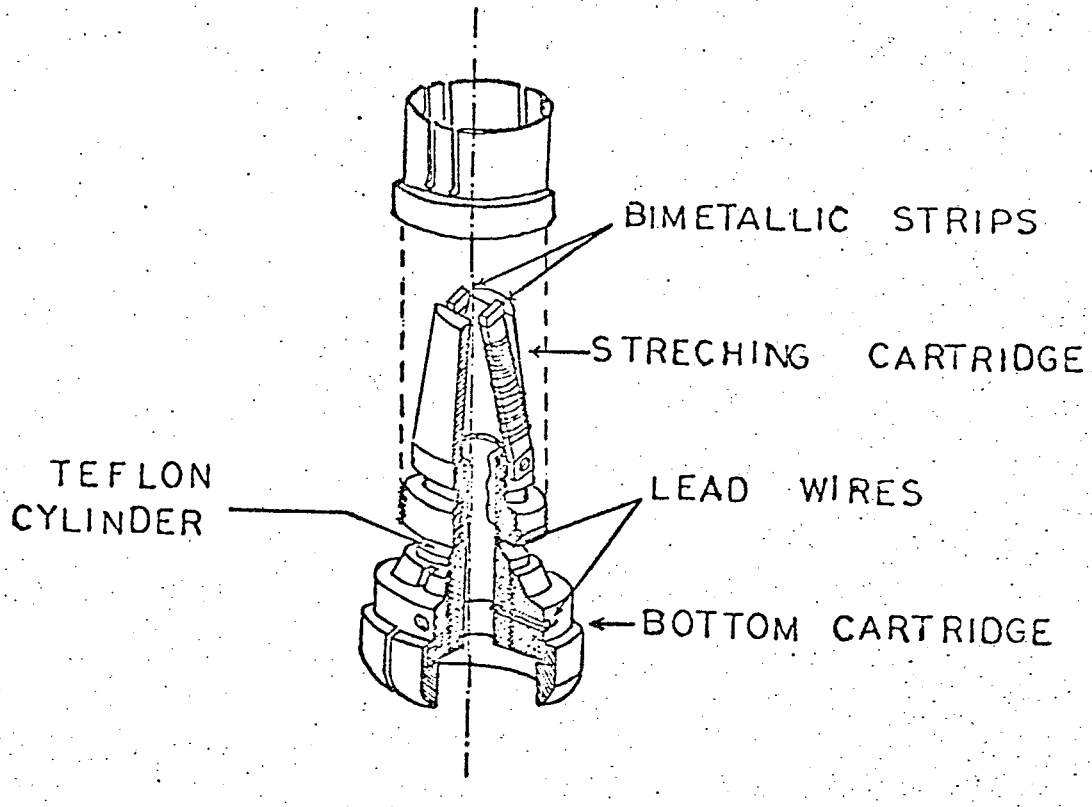

Figure 15 MICRO TENSILE DEVICE

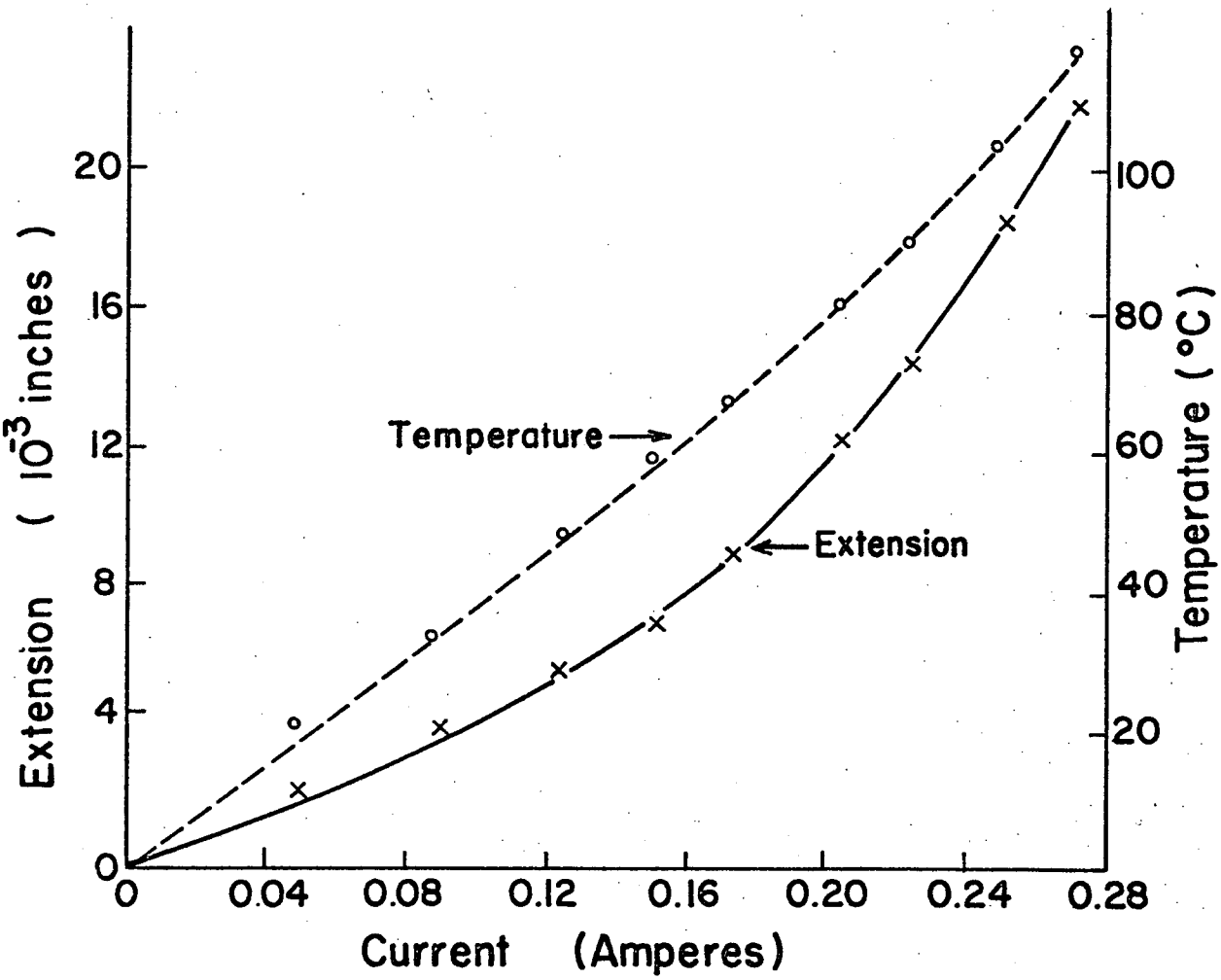

Figure 16: Relation between the heater current, temperature, and extension of the bimetallic strips of the microtensile device.

cartridges are made of phosphor-bronze. The insulation between the stretching cartridge and the bottom cartridge was achieved by mounting them on a Teflon cylinder with appropriate spacings. One of the leads of the winding is grounded to the body of the microscope through the bottom cartridge. The other lead is connected to a steel ring mounted between the stretching and bottom cartridges on the bottom cylinder, to which current is fed through a contacting socket in the hot stage plate, kept insulated from the rest of the stage. The strip temperature is measured by a thermocouple attached to the end of the strips. The strain induced by heating the strips was determined by optically measuring the spacing between the strips as a function of heater current and strip temperature. A maximum current of 0.27 amperes corresponds to a maximum deflection of 21.75×10^{-3} inches at a temperature rise of about 117°C. The initial spacing of the bimetallic strips is adjustable. For a 1 mm. initial spacing the maximum overall strain that could be imposed on the thin foil sample is 50% with an accompanying temperature rise to 100°C. The relationship between the heater current, temperature and extension of the bimetallic strips is shown in Fig. 16. The design, construction and set-up of the tensile strain device was completed near the end of the contract period and as a result did not permit its utilization for the intended study.

(8) ANALYSIS OF STRESS FIELD PERTURBATION BY DISPERSED PARTICLES

Earlier investigation[19,1,24] suggested that particle-martix interface decohesion can influence the yielding and fracture behavior of two phase materials. Here the decohesion of the particle-matrix interface is controlled by the normal stress distribution across the interface resulting from the elastic discontinuity during loading and from the thermo-mechanical processing history of the material, which includes the stresses introduced due to differential thermal contraction of the particle and the matrix.

These effects have had a particular impact on TD-Nickel and TD-Nichrome systems in terms of the observation of their sensitivity to thermo-mechanical history on their mechanical behavior, displaying a strength differential effect in some heats of the former, and the appearance of reduced high temperature yield strengths following rapid heating for both alloys. In view of the above, an analysis of the interface behavior under the combined stress field is considered.

The method involves evaluating the normal stress distributions across the interface due to elastic discontinuity and thermal history from Goodyear's[25] and Mott & Nabarro[26] treatments respectively and combining them through a non-dimentional parameter, β , whose value can be estimated for a material with known dispersoid and thermal history. The analysis is presented in the following pages.

PERTURBATION OF STRESSES AROUND A SPHERICAL INCLUSION UNDER UNIFORM TENSION T_A:

I. Spherical co-ordinates (Goodier's solution)

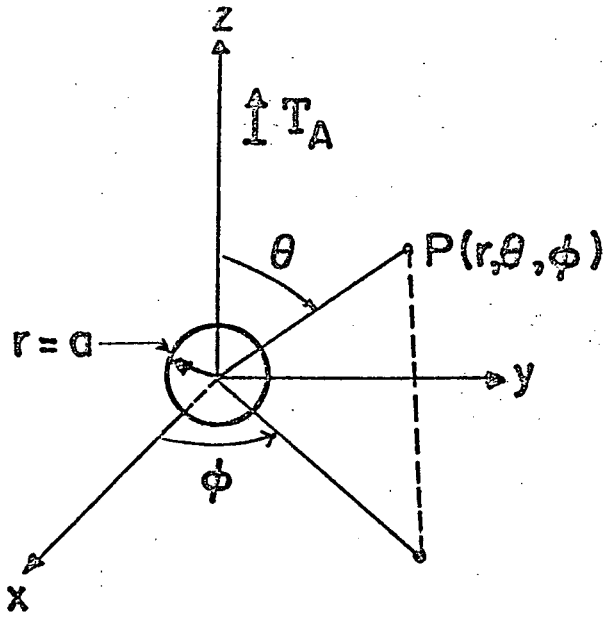

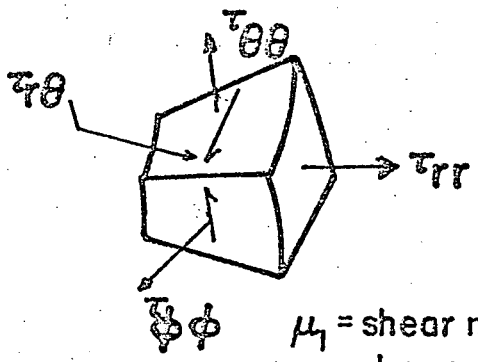

μ_1 = shear modulus of matrix
μ_2 = shear modulus of inclusion
σ_1 = poison ratio of matrix
σ_2 = poison ratio of inclusion
a = radius of inclusion

$$\tau_{rr} = 2\mu_1\left\{\left[\frac{2A}{r^3} - \frac{2\sigma_1}{1-2\sigma_1}\frac{c}{r^3} + \frac{12B}{r^5}\right] + \left[36\frac{B}{r^5} - \frac{2(5-\sigma_1)}{1-2\sigma_1}\frac{c}{r^3}\right]\cos 2\theta\right\} + \frac{T_A}{2}(1+\cos 2\theta$$

$$\tau_{\theta\theta} = 2\mu_1\left\{\left[-\frac{A}{r^3} - \frac{2\sigma_1 c}{1-2\sigma_1 r^3} - \frac{3B}{r^5}\right] + \left[\frac{c}{r^3} - 21\frac{B}{r^5}\right]\cos 2\theta\right\} + \frac{T_A}{2}(1-\cos 2\theta)$$

$$\tau_{\phi\phi} = 2\mu_1\left\{\left[-\frac{A}{r^3} - \frac{2(1-\sigma_1)}{1-2\sigma_1}\frac{c}{r^3} - 9\frac{B}{r^5}\right] + \left[3\frac{c}{r^3} - 15\frac{B}{r^5}\right]\cos 2\theta\right\}$$

$$\tau_{r\theta} = 2\mu_1\left[-\frac{2(1+\sigma_1)}{1-2\sigma_1}\frac{c}{r^3} + 24\frac{B}{r^5}\right]\sin 2\theta - \frac{T_A}{2}\sin 2\theta$$

where the values of constants A,B and C are given by :

$$\frac{A}{a^3} = -\frac{T}{8\mu_1(7-5\sigma_1)\mu_1 + (8-10\sigma_1)\mu_2} \times \frac{(1-2\sigma_2)(6-5\sigma_1)2\mu_1 + (3+19\sigma_2 - 20\sigma_1\sigma_2)\mu_2}{(1-2\sigma_2)\mu_1 + (1+\sigma_2)\mu_2}$$

$$+ \frac{T}{4\mu_1} \frac{\left[(1-\sigma_1)\ \frac{1+\sigma_2}{1+\sigma_1} - \sigma_2\right]\mu_2 - (1-2\sigma_2)\mu_1}{(1-2\sigma_2)2\mu_1 + (1+\sigma_2)\mu_2}$$

$$\frac{B}{a^5} = \frac{T}{8\mu_1} \frac{\mu_1 - \mu_2}{(7-5\sigma_1)\mu_1 + (8-10\sigma_1)\mu_2}$$

$$\frac{C}{a^3} = \frac{T}{8\mu_1} \frac{5(1-2\sigma_1)(\mu_1 - \mu_2)}{(7-5\sigma)\mu_1 + (8-10\sigma_1)\mu_2}$$

THERMAL STRESSES FROM PROCESSING

DIFFERENTIAL THERMAL CONTRACTION MISMATCH

$$\delta = \left[\frac{1+\alpha_2 \Delta T}{1+\alpha_1 \Delta T}\right] - 1$$

ACCOMPANYING STRAINS

$$e_{rr} = \frac{2\epsilon a^3}{r^3} \qquad e_{\theta\theta} = e_{\phi\phi} = -\frac{\epsilon a^3}{r^3}$$

WHERE

$$\epsilon = \frac{3\mu_2 \delta}{3\mu_2 + \left[2E_1/(1+\sigma_1)\right]}$$

ASSOCIATED RADIAL STRESS COMPONENT

$$\tau = \frac{2E_1 \epsilon}{1+\sigma_1}\left(\frac{a}{r}\right)^3$$

STRESSES ACROSS THE INTERFACE

I. DUE TO ELASTIC DISCONTINUITY

(Rigid inclusion $\mu_1/\mu_2=0$, metal matrix $\sigma_1=1/3$)

$$\tau_{rr}=\frac{T_A}{2}\left\{\left[1+2\left(\frac{a}{r}\right)^3-\frac{9}{7}\left(\frac{a}{r}\right)^5\right]+\left[1+5\left(\frac{a}{r}\right)^3-\frac{27}{7}\left(\frac{a}{r}\right)^5\right]\cos 2\theta\right\}$$

II. DUE TO THERMAL HISTORY

$$\tau_{rr}=\frac{6\mu_2 E_1\delta}{3\mu_2(1+\sigma_1)+2E_1}\left(\frac{a}{r}\right)^3 \doteq \frac{3}{2}E_1\epsilon\left(\frac{a}{r}\right)^3$$

III. COMBINED STRESSES

For a nondimensional parameter $\beta=\frac{M}{T_A}$, where $M=\frac{3}{2}E_1\epsilon$;

normal stress across interface ($r=a$) reduces to:

$$\tau_{rr}=\frac{T_A}{2}\left(\frac{12}{7}-2\beta+\frac{15}{7}\cos 2\theta\right)$$

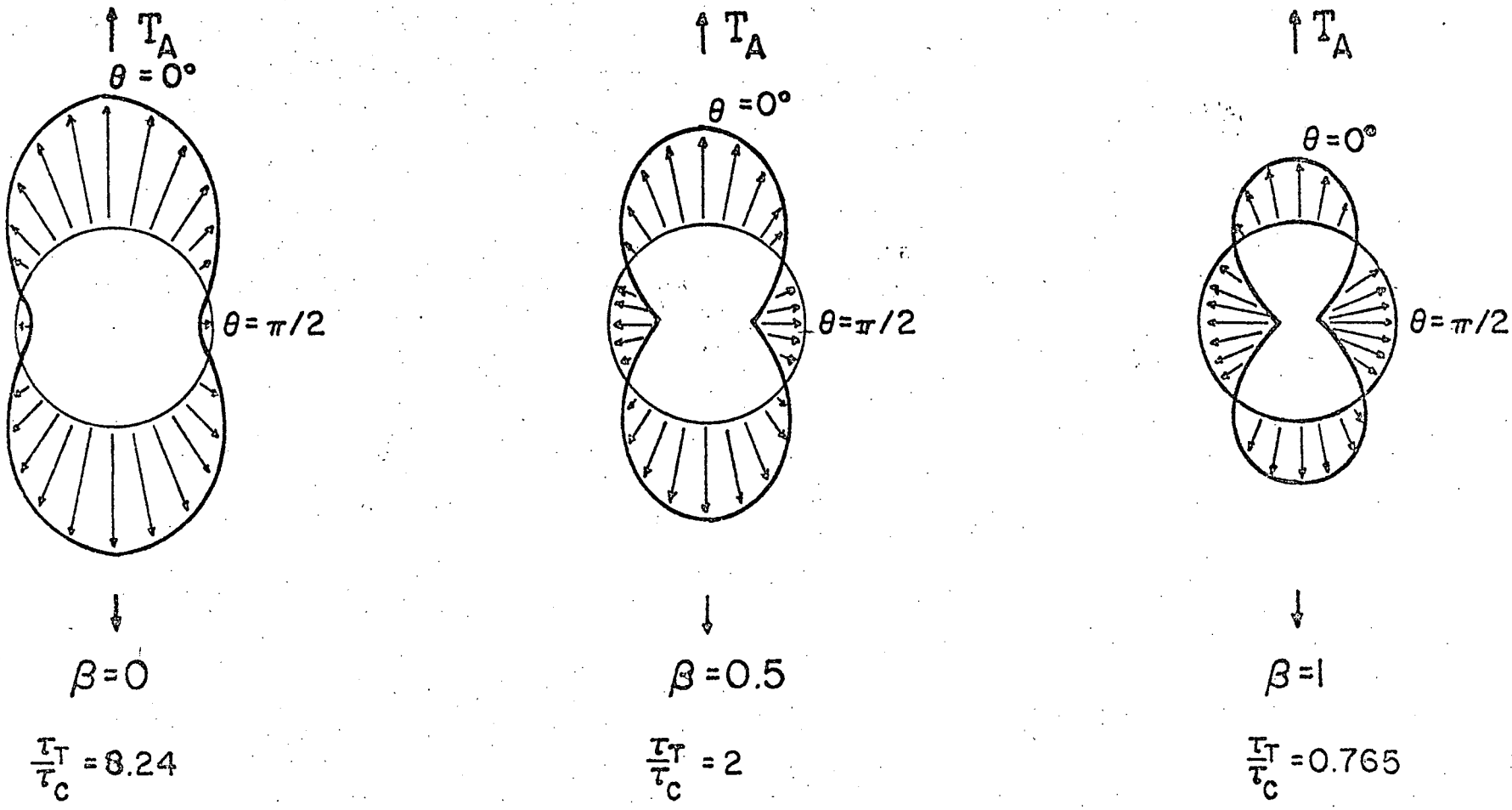

DISTRIBUTION OF NORMAL STRESSES ACROSS THE INTERFACE

For this case of TD-Nickel the value of the parameter β lies in the neighborhood of 1.65. The consequence of this is that for cases where the processing history can impose its full potential stress field, the particle-matrix interface decohesion can be fully suppressed. This in fact explains the processing sensitiveness of the SD effect in these materials and the suspected lack of reproducibility of SD effect from heat to heat as commented by Wilcox et al[27] recently.

The next aspect that has been considered is the nature of dislocation-particle interaction under applied load and its consequences on the particle by-pass mechanism of a dislocation in a dispersion-strengthened system. The perturbation of stress field around a second phase particle due to elastic discontinuity could considerably influence the particle by-pass mechanism, and a greater understanding of this would help in formulating the yielding creiteria in these systems.

In addition to the inhomogeneity interaction due to unbalanced relaxation of its stress field, a dislocation approaching a particle will also encounter the 'equivalent inclusion interaction' which is essentially due to the perturbation of the externally applied stress field around the particle.

The inhomogeneity interaction can be estimated by Eshelby's[28] method as pointed out by Ashby[29] but only for a long range interaction while the image force treatment is more appropriate when we consider the interaction of a dislocation within about two diameters from the inclusion.

i.e. the inclusion interactions are given by:

for $r \geq 5a$ $$E_{int} = -\tfrac{1}{2}V\left\{\frac{A}{9k_1}\, pp + \frac{B}{2\mu_1}\, {}'p_{ij}\,{}'p_{ij}\right\}$$

and for $5 \leq 2a$ $$2a\ E_{int} = \mu_1\left(\frac{\mu_2 - \mu_1}{\mu_2 + \mu_1}\right)\frac{b^2}{2\pi r}$$

where $$A = \frac{K_2 - K_1}{1/3\left(\frac{1+\sigma_1}{1-\sigma_1}\right)\left(K_2 - K_1\right) + K_1} \qquad B = \frac{\mu_2 - \mu_1}{2/15\left(\frac{4-5\sigma_1}{1-\sigma_1}\right)\left(\mu_2 - \mu_1\right) + \mu_1}$$

K_1 and K_2 are the bulk modulei of the matrix and the inclusion respectively

and $p = p_{11}+p_{22}+p_{33}$ ${}'p_{ij} = p_{ij} - 1/3\ {}_{ij}\, p$ the stress components of the dislocation.

The 'equivalent inclusion interaction' at distances greater than about five diameters from the inclusion is only due to resolved shear stress from the external load, while at distances with in five diameters from the inclusion the interaction is due to the stresses associated with the perturbation around the particle. The stress distribution associated with the perturbation can be obtained in spherical co-ordinate system from Goodyear's[25] solution as shown before. But in order to be able to evaluate the nature of interaction of a dislocation approaching a particle on a set of slip planes at a specific orientation with the direction of the applied load, we need to evaluate the glide components of the stress field on the slip planes. This is achieved by suitably transforming the components in the spherical co-ordinate system to a rectangular co-ordinate system followed by a rotation to match the slip system. A diagramatic view of the analysis is indicated in the next page.

STRESS COMPONENTS IN THE PRIMARY SLIP SYSTEM

TRANSFORMATION: $\tau_{ij} = \alpha_{ik}\alpha_{jl}\tau_{kl}$

SPHERICAL
(r, θ, ϕ)

CARTESIAN
(x, y, z)

CARTESIAN
(PRIMARY SHEAR)
(x', y', z') $\eta = \pi/4$

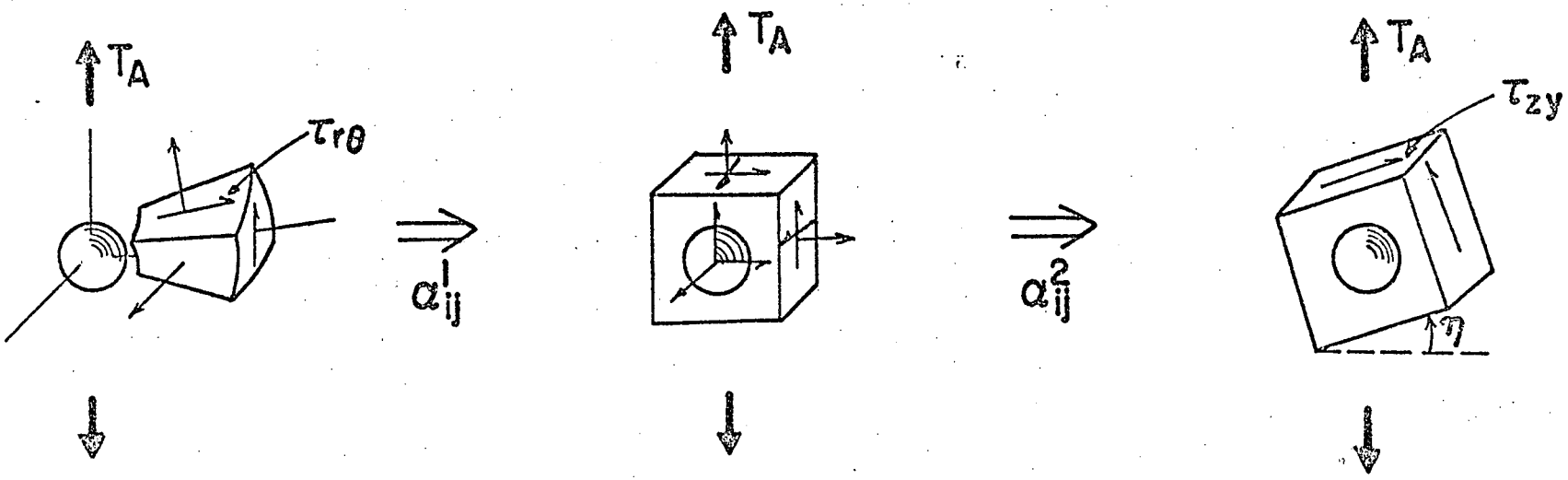

$$\alpha^1_{ij} = \begin{bmatrix} \sin\theta\cos\phi & \cos\theta\cos\phi & -\sin\phi \\ \sin\theta\sin\phi & \cos\theta\sin\phi & \cos\phi \\ \cos\theta & -\sin\theta & 0 \end{bmatrix}$$

$$\alpha^2_{ij} = \begin{bmatrix} 1 & 0 & 0 \\ 0 & \cos\eta & \sin\eta \\ 0 & -\sin\eta & \cos\eta \end{bmatrix}$$

The transformation and plotting of the glide components of the stress functions on the set of slip planes for edge and screw dislocations is done with the help of computer.

The nature of the distribution of these glide stress components for screw and edge dislocations is quite interesting. Based on these, an attempt is now being made to evaluate the dislocation bowing shapes and to predict the particle by-pass mechanisms in a dispersion strengthening system.

More work needs to be done along these lines to understand the basic mechanism and evlauate the yielding creiteria in these systems.

CONCLUSIONS

1. The particle-matrix interface strength of TD-Nichrome sheet was measured to be between 198,000 psi and 238,000 psi. This is about five times the interface strength measured by Rao et al[13] for TD-Nickel.

2. The heat of TD-Nichrome tested did not exhibit an SD effect. However, the occurrence of an SD effect appears to vary for different heats within the same alloy system.

3. It appears that rapid heating causes interface decohesion both TD-Nickel and TD-Nichrome. This was illustrated by the change in appearance of the fracture surface of TD-Nichrome with time at temperature.

4. The combination of fast thermal shock together with externally applied load can cause premature failure during high temperature stress-rupture and creep testing as compared with conventional test results.

5. Analysis of the stress distribution in two phase alloys indicates that both of thermal and external load induced stresses can in combination act either to cause or to retard interface rupture depending upon the thermal and stress histories and the physical properties of the phases.

REFERENCES

1. Olsen, R. J. and Ansell, G. S., "The Strength Differential in Two-Phase Alloys", Trans. ASM, 62, 711 (1969).

2. Olsen, R. J., Judd, G., and Ansell, G. S., "Measurement of Particle-Matrix Interface Strength in TD-Nickel", Met. Trans., 2, 1353 (1971).

3. Leslie, W. C. and Sober, R. J., "The Strength of Ferrite and of Martensite as Functions of Composition, Temperature, and Strain Rate", ASM Trans. Quart., 60, 459 (1967).

4. Rauch, G. C. and Leslie, W. C., "The Extent and Nature of the Strength-Differential Effect in Steels", to be published.

5. Feisel, O. H., as reported by Leszynski, W. (ed.), Powder Metallurgy, Interscience, New York, 306 (1961).

6. McEvilvy, A. J., Ku, R. C., and Johnston, T. L., "The Source of Martensite Strength", Trans. AIME, 236, 108 (1966).

7. Patel, J. R. and Cohen, M., "Criterion for the Action of Applied Stress in the Martensitic Transformation", ACTA Met., 1, 531 (1953).

8. Rauch, G. C., Daga, R. L., Radcliffe, S. V., Richmond, O., Sober, R. J., and Leslie, W. C., "Volume Expansion, Pressure Effects, and the Strength Differential in Iron-Carbon Martensites", to be published.

9. Hirth, J. P., and Cohen, M., "On the Strength-Differential Phenomenon in Hardened Steel", Met. Trans., 1, 3 (1970).

10. Orowan, E., "Symposium of Internal Stresses in Metals and Alloys", J. Inst. Metals, 451 (1948).

11. Ansell, G. S., "The Mechanism of Dispersion Strengthening: A Review", Oxide Dispersion Strengthening, G. S. Ansell, T. D. Cooper, and F. V. Lenel (eds.), Gordon and Breach, New York, 61 (1968).

12. Ashby, M. F., "The Theory of the Critical Shear Stress and Work Hardening in Dispersion-Hardened Crystals", Harvard Univ. Tech. Rept. No. 515, Office of Naval Research, Contract NONF-1866(27), (December 1966).

13. Rao, G., Olsen, R. J., Judd, G., and Ansell, G. S., Met. Trans. V. 3, 737 (1972).

14. Kingery, W. D., Property Measurements at High Temperatures, John Wiley and Sons, New York (1959).

15. Weast, R. C. (ed.), Handbook of Chemistry and Physics, Chemical Rubber Publishing Co., Cleveland (1962).

16. Olsen, R. J., "The Strength Differential Effect in Two-Phase Alloys", Ph.D. Thesis, Rensselaer Polytechnic Institute, 1970.

17. Lyman, Taylor (ed.), Metals Handbook,vol. 1, Amer. Soc. Metals, Ohio (1961).

18. Savage, W. F. "Apparatus for Studying the Effects of Rapid Thermal Cycles and High Strain Rates on the Elevated Temperature Behavior of Materials", J. Appl. Polymer Science, VI, 303 (1962).

19. Palmer, I. G. and Smith, G. C., "Fracture of Internally Oxidized Copper Alloys", Oxide Dispersion Strengthening, G. S. Ansell, T. D. Copper, and F. V. Lenel (eds.), Gordon and Breach, New York, 61 (1968).

20. Webster, D., "Microvoids Influence Metal Properties", Metals Progress, 93, 1, 93 (1968).

21. Tetelman, A. S. and McEvilvy, A. J., Fracture of Structural Materials, John Wiley and Sons, New York, 110 (1967).

22. Spinner, S., Knudson, F. P., and Stone, L., "Elastic Constants-Porosity Relations for Polycrystalline Thoria", J. Res. Nat. Bur. Std., 67C 39 (1963).

23. Lang. S. M., "Properties of High-Temperature Ceramics and Cermets; Elasticity and Density at Room Temperature", Nat. Bur. Std. Monograph #6 March, 1960.

24. Gurland, J. and Plateau, J., Trans. ASM, 1963, vol. 56, p. 442.

25. Goodier, J. N., J. Appl. Mech., 1933, vol. 55, p. 39.

26. Mott, N. F. and Nabarro, F. R. N., Proc. Phys. Soc. 1940, vol. 52, p. 86.

27. Wilcox, B. A. Clauer, A. H. and Luetjering, G., Trans. ASM, 1972, vol. 3, p. 1666.

28. Eshelby, J. D., Proc. R. Soc. 1957, A241, p. 376.

29. Ashby, M. F. et. al, Acta Met. 1969, vol. 17, p. 1403.